

Contents

Introduction	iii
1 Production and processing of resonant cavities: an innovative solution	1
1.1 <i>Seamless cavity production</i>	1
1.2 <i>Traditional surface treatments</i>	3
1.2.1 <i>Mechanical Polishing, BCP, EP</i>	4
1.2.2 <i>Helium Processing</i>	5
1.2.3 <i>Heat treatment of niobium cavities</i>	6
1.2.4 <i>High pressure rinsing</i>	6
1.2.5 <i>High power pulsed rf processing</i>	7
1.3 <i>A new chance: atmospheric plasma cleaning</i>	7
2 Industrial atmospheric plasma treatments	9
2.1 <i>Introduction</i>	9
2.1.1 <i>Plasmas classification</i>	10
2.1.2 <i>Overview of various atmospheric plasma sources</i>	12
2.2 <i>Examples of industrial applications</i>	17
2.2.1 <i>Textile</i>	17
2.2.2 <i>Bottles and Displays</i>	26
3 Radio-frequency atmospheric plasma cleaning applied to niobium resonant cavities	31
3.1 <i>Experimental details</i>	31
3.1.1 <i>rf apparatus</i>	31
3.1.2 <i>Cryogenic infrastructure</i>	35
3.1.3 <i>Procedure</i>	44
3.2 <i>1.5 GHz cavities</i>	45
3.3 <i>6 GHz cavities</i>	47
4 Discussion	51
5 Conclusions and future plan	55
A Basics of superconducting radio-frequency cavities	57
A.1 <i>Cavity fundamentals and cavity fields</i>	57
A.1.1 <i>Radio-frequency fields in cavities</i>	57
A.1.2 <i>The accelerating field</i>	58
A.1.3 <i>Peak surface fields</i>	59

A.1.4 <i>Power dissipation and the cavity quality</i>	60
List of Tables	63
List of Figures	65
BIBLIOGRAPHY	69

Introduction

Preparation of cavity walls has been one of the major problems in superconducting radio-frequency (SRF) accelerator technology. Accelerator performance depends directly on the physical and chemical characteristics at the SRF cavity surface.

The ambitious objective of this project is to study a cavity surface preparation process which is superior in terms of cost, performance, and safety, to the wet chemical process currently in use. Plasma based processes provide an excellent opportunity to achieve these goals.

Plasmas are chemically active media. Depending on the way they are activated and their working power, they can generate low or very high "temperatures" and are referred correspondingly as cold or thermal plasmas. This wide temperature range enables various applications for plasma technologies: surface coatings, waste destruction, gas treatments, chemical synthesis, machining ... many of these techniques have been industrialized. A large number of important industrial plasma applications are carried out close to atmospheric pressure, in many cases in atmospheric air.

The fascinating possibility to perform cleaning and/or etching processes of RF cavities without the need of any vacuum pumping system has to be deeply explored realizing different atmospheric configurations as corona plasma, rf resonance plasma, plasma jet and torch.

Thermal plasmas (especially arc plasma) were extensively industrialized, principally by aeronautic sector. Cold plasma technologies have been developed in the microelectronics but their vacuum equipment limits their implantation.

To avoid drawback associated with vacuum, several laboratories have tried to transpose to atmospheric pressure processes that work under vacuum for the moment. Their researches have led to various original sources.

In the textile sector, a number of plasma applications are conceivable and some have been tested in laboratory scale. The chemical functionality and/or the morphology of a fiber surface can be altered in order to improve very different properties to tailor them for certain demands. The wettability can be increased to achieve a better impregnation or a deeper dyeing or, in contrast; it also can be decreased to create a water repellent behavior. New chemical functionalities on the surface can promote the reactivity with dyes. The ad-

hesion in laminates can be enhanced largely. The water free removal of sizings seems to be possible. These are only a few examples that demonstrate the potential of this technology.

We decided to try to ignite a resonance atmospheric plasma into 1.5 GHz superconducting niobium cavities to perform a feasibility study. The second step has been the attempt to understand what really happens to the resonant structure internal surface. The most powerful tool consists in the atmospheric plasma treatment and fast rf characterization of 6 GHz small resonators.

Chapter 1

Production and processing of resonant cavities: an innovative solution

This chapter attempts to give an overview of production and processing of niobium resonant cavities. At first the spinning process is briefly described. In the second part the surface treatments associated with cavities are presented. Not only mechanical smoothing, chemical and electrochemical polishing but also the surface treatments that have been found to be effective in suppressing field emission are reported: helium processing, heat treatments, high pressure rinsing and high power pulsed rf processing. The ambitious objective of this project is to start studying an innovative cavity surface preparation process based on rf resonance plasma at atmospheric pressure.

1.1 *Seamless cavity production*

The spinning process has been developed at INFN-LNL.

Seamless cavities can be cold formed at a rate of almost one cell per hour, by spinning a simple circular blank onto a suitable mandrel (figure 1.1). No matter the number of cells, no intermediate annealing is required. The mandrel is made collapsible to permit easy extraction from the cavity once the spinning process is finished. The extraction of the mandrel parts from the cavity generally takes a few minutes, depending on the complexity of the cavity shape. The presence of an internal mandrel permits very tight tolerances. As a consequence, the resonant frequency distribution of spun cells has a low standard deviation. The material elongation limit is of minor importance because the material is plastically displaced along all three dimensions.

If a larger blank is chosen, a multi-cell cavity can easily be spun too. Also in this case no intermediate annealing is required. 9-cell copper and niobium cavities (Tesla Type) have been obtained. Spinning a multi-cell cavity from a disk is possible, but it is not practical for industrial production. In this case, the blank is initially spun into a conic frustum.



Figure 1.1: A seamless Tesla Type bulk niobium 6 GHz cavity. Spun resonators don't need welding (even for flanges).

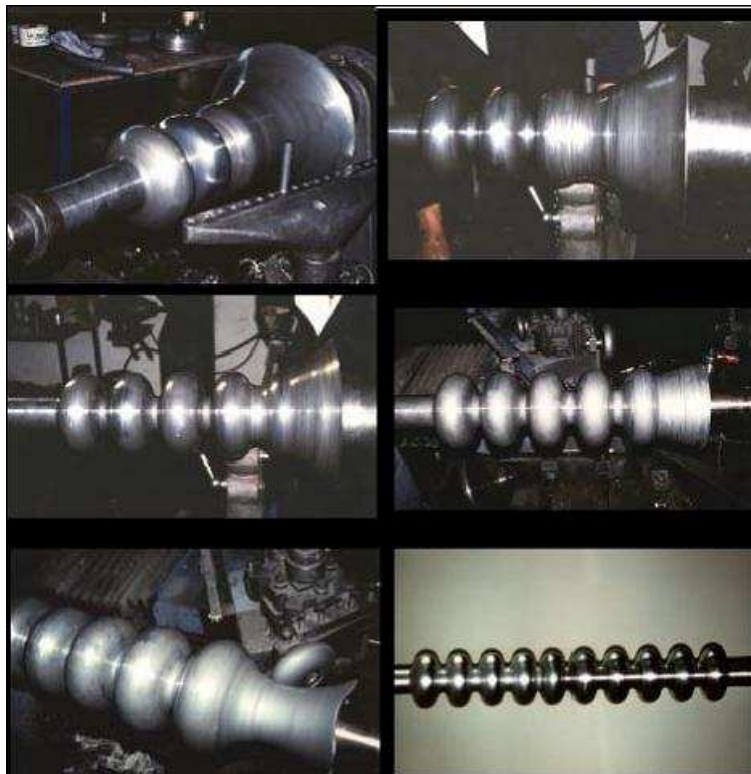


Figure 1.2: Spinning of a seamless multicell resonator from a circular blank.

It is much more convenient to spin a multicell cavity from a tube, because the spinning procedure is the same for every cell.

1.2 *Traditional surface treatments*

The surface treatments associated with cavities is a key issue towards the obtaining of high performance. Standard surface treatments involve mechanical polishing, chemical or electrochemical polishing, rinsing procedures and baking. Electropolishing is believed to provide the highest accelerating gradients (compared to chemical polishing).

In order to reach the desired accelerating field and Q_0 factor, niobium cavities go through different surface treatments after their delivery by industry:

- Chemical and/or electrochemical polishing: 150 μm of niobium are stripped out.
- High Pressure Rinsing (HPR) with ultra-pure water.
- Baking (110°C, 48h).
- Final Assembly inside clean environment (class 10-100 cleanroom).

In order to achieve efficient cavity preparation (avoiding particle contamination of the inner surface), laboratories tend to implement at the same place treatments units and clean rooms, where they are mounted. Cavities are then tested in a cryostat.

However, for a number of reasons, the highest possible accelerating gradients are never achieved in practical cavities. The most common limiting mechanisms are field emission, thermal breakdown, and multipacting.

Field emission is the primary mechanism that limits the accelerating gradients of present day cavities. In the presence of a high surface electric field, rf power is lost to electrons that tunnel out of the cavity wall at very localized points. The emitted electrons are accelerated by the electromagnetic fields and, upon impact, heat the cavity wall and produce x-rays. Field emission scales exponentially with the electric field and is capable of consuming inordinate amounts of power.

Thermal breakdown generally results when a highly resistive defect on the rf surface causes a large fraction of the cavity to quench. An abrupt reduction of the cavity quality results. Thermal breakdown can also be initiated by the heat from bombarding field emission electrons.

Multipacting is a resonant process, in which a large number of electrons build up an avalanche by repeated impact with the cavity walls. Again, the heat deposited by these impacts can lead to thermal breakdown. In the absence of thermal breakdown, the absorption of rf power by multipacting electrons can still make it impossible to raise the cavity fields.

Even at low field levels (below an accelerating gradient of a few MV/m) all cavities display losses higher than theoretically expected. The anomalous losses are attributed to a temperature independent residual resistance. The dominant sources for this resistance are

impurities on the rf surface, adsorbed gases, and residual magnetic flux that is trapped in the superconductor as it is cooled through the transition temperature. In some cases the precipitation of niobium hydride at the rf surface due to hydrogen stored in the wall may also contribute to the residual resistance. This phenomenon is known as the "Q-virus", and it can be avoided by driving out the hydrogen during a vacuum bake of the cavity at 900°C.

1.2.1 *Mechanical Polishing, BCP, EP*

Mechanical Polishing

To improve the yield of the niobium accelerator cavities that satisfies required performance, it is important to apply mechanical grinding as a pre-treatment before chemical polishing.

It is done using a *tumbler*: the resonator to be treated is filled with a certain number of abrasive agent pieces (media), plugged up and fixed to the machine. The tumbler makes the cavity rotate so that the media pieces can erode the metal surface in a uniform, controllable and reliable way. The materials used for this kind of mechanical polishing are: SiC, Al₂O₃ and ZrO₂.

Buffered chemical polishing (BCP)

Metal surface is treated with a mixture of nitric (oxidizing specie), sulfuric and phosphoric acids. Cavities might be plunged in an acid bath or treated internally thanks to a close circuit. This technique provides a fast niobium removal rate (1 μm.mn⁻¹ or higher) but the surface is etched at grain boundaries and is then not very smooth.

NO₃⁻ ion makes niobium oxidize into its state +5. NO₃⁻ is reduced into NO_x:

- NO₃⁻ + 4H⁺ + 3e⁻ → NO + 2H₂O
- 2Nb + 5H₂O → Nb₂O₅ + 10e⁻ + 10H⁺
- 6Nb + 10HNO₃ → 3Nb₂O₅ + 10NO + 5H₂O

In presence of HF, Nb₂O₅ is transformed into fluoride or oxifluoride species:

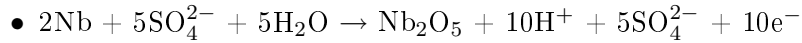
- Nb₂O₅ + 14HF → 2H₆NbO₂F₇ + H₂O
- Nb₂O₅ + 12HF → 2HNbF₆ + 5H₂O
- Nb₂O₅ + 10HF → 2NbF₅ + 5H₂O
- Nb₂O₅ + 10HF → 2H₂NbOF₅ + 3H₂O
- HNbF₆ + HF → H₂NbF₇

Electropolishing

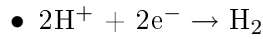
This technique that we will discuss in this report provides smooth surfaces with lower roughness and higher E_{acc} . Surface smoothness is believed to be the origin of the cavity performance. But that question is not totally elucidated.

The electrolyte that is used is composed of hydrofluoric (40 w%) and sulfuric (96 w%) acids in a ratio: 1 volume HF for 9 volumes of H_2SO_4 . The bath temperature is controlled in order to stabilize at about 30 °C leading current densities between 30 and 100 mAcm^{-2} . The cathode is made of aluminum.

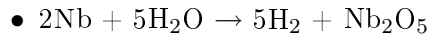
Niobium oxidation during electropolishing might be written:



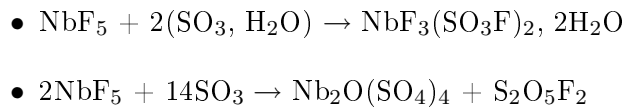
The reduction process is hydrogen formation at the aluminum cathode:



For a global and easier understanding, the oxido-reduction equation might be written:



Nb_2O_5 is then dissolved to form niobium fluoride, oxofluoride species and fluorosulfate or oxysulfate and pyrosulfuryfluoride because of sulfuric acid considered as hydrated sulfur trioxide (SO_3 , H_2O):



1.2.2 Helium Processing

In this method [1] helium gas at low pressure (10^{-5} torr, or just below discharge threshold) is admitted into a *cold* superconducting cavity. The cavity is operated near the maximum possible field level for several hours. There are some indication of *field emission reduction*. In high frequency (> 1000 MHz) cavities, performance improvement occurs during the first few minutes. In low frequency cavities, gains continue over periods between 1 and 50 hours.

As an example, the results on a series of 1-cell 1.5 GHz cavities showed a gain of about 30% at $E_{pk} = 20\text{-}30$ MV/m (that decreased to 10% at 50-60 MV/m) [1].

Helium processing was also found to be effective in suppressing field emission from an emitter source introduced intentionally: carbon flakes deliberately placed on the superconducting cavity surface. This studies have clearly established the usefulness of helium processing.

Experiments show that helium processing works in a number of different ways, or perhaps in a combination of ways. It has been established that at least part of the benefit comes from removal of gas condensates. Emitters activated by deliberately condensing

gas were identified by thermometry and subsequently removed by helium processing. One expects that condensate changes would be realized by helium ion bombardment and in a short period of time (minutes). Another result showed that admission of helium triggers a microdischarge at a field emission site. If the field level is not high enough for rf processing, the presence of helium gas will help to initiate the discharge which subsequently destroys the emitter. We expect that this effect should proceed quickly, probably immediately after admitting sufficient helium gas into the cavity.

Helium processing over time periods of many tens of hours is also known to reduce field emission. This effect has traditionally been interpreted as sputtering of the bulk emitter over longer periods of time. Long time helium processing is more effective for low frequency cavities because of the higher impact energy of the helium ions and the higher sputtering rate.

Another mechanism has been suggested for the effectiveness of helium processing. In a series of studies on dc field emission from copper surfaces, room temperature, high voltage conditioning experiments have been carried out in the presence of a variety of gases, including helium. The results of these studies have been interpreted as ion implantation that alters the emitter properties [1].

1.2.3 *Heat treatment of niobium cavities*

The influence of high temperature annealing in the final stage of rf cavity surface preparation has been studied [1]. Heat treatment to eliminate field emission should not be confused with heat treatment for postpurification, where the rf surface and the exterior of a niobium cavity are surrounded by titanium as the solid state gettering agents and where the rf surface is etched after HT to remove the evaporated layer.

For the superconducting cavities, the most significant reduction in field emission was observed for 4 to 8 hours heat treatments at 1400-1500°C. A corroboration of the benefit of HT comes from the temperature maps: many strong emitters are seen when the standard chemical treatment is used, whereas the HT surfaces are virtually free of emitters at 30 MV/m.

The potential benefits of a new treatment indicated by sample tests or single cell cavity tests, must always be checked on a large area, multicell cavity: the mixed experience with HT on multicell cavities indicates that it is indeed difficult to keep large area multi cell cavities clean on a reproducible basis.

1.2.4 *High pressure rinsing*

Field emitter studies [1] shows that increased vigilance in cleanliness during final surface preparation and assembly procedures is important to keep particulate contaminations and associated emission under control [2, 3, 4].

A technique to improve cleanliness that is high pressure water rinsing (HPR): a jet of

ultrapure water is used to dislodge surface contaminants resistant to conventional rinsing procedures.

The benefits of HPR in reducing field emission are well demonstrated.

1.2.5 *High power pulsed rf processing*

While the supercleanliness approach of HPR has unarguable potential, but a single field emission site can degrade the Q_0 of a superconducting cavity, if the emitter will not process away at the maximum rf power available. In large area structures there is always a significant probability that a few emitters will find their way onto the cavity surface. This is the reason why the maximum achievable field decreases with the cavity area. There is also the danger of dust falling into the cavity during installation of power coupling devices.

Therefore a technique that eliminates emitters in situ is highly desirable for successful application of superconducting cavities to accelerators. Such a technique has been developed and it is called High Pulsed Power processing (HPP) [5, 6].

The essential idea of high power rf processing an emission site is to rise the surface electric field at the emitter as high as possible, even for a very short time ($\ll \mu s$). As the field rises, the emission current rises exponentially to the level at which melting, evaporation, gas evolution, plasma formation and a microdischarge take place. The ensuing explosive event destroys the emitter.

1.3 *A new chance: atmospheric plasma cleaning*

As already mentioned, preparation of cavity walls has been one of the major problems in superconducting radio-frequency (SRF) accelerator technology. Accelerator performance depends directly on the physical and chemical characteristics at the SRF cavity surface. The ambitious objective of this project is to start studying a cavity surface preparation process which is superior in terms of cost, performance, and safety, to the wet chemical process currently in use. Plasma based processes provide an excellent opportunity to achieve these goals.

A large number of important industrial plasma applications are carried out close to atmospheric pressure, in many cases in atmospheric air.

The *fascinating possibility* to perform cleaning and/or etching processes of RF cavities without the need of any vacuum pumping system has to be deeply explored realizing different atmospheric configurations as corona plasma, rf resonance plasma, plasma jet and torch.

We decided to start the investigation from the rf resonance plasma: it is simple, reliable and easy to set up. It becomes possible to:

- Clean the Nb surface from carbon contamination or adsorbed gases
- Etch the Nb surface using plasma activated chemicals
- Add an efficient cleaning step to the surface treatments of cavities

- Substitute dangerous steps of Nb cavity chemistry

Chapter 2

Industrial atmospheric plasma treatments

This chapter attempts to give an overview of atmospheric plasma sources and their applications. In a first part the main scientific background concerning plasmas will be introduced while the second part focuses on the various applications of the atmospheric plasma technologies, mainly in the field of surface treatments [7].

2.1 Introduction

Plasma is a more or less ionized gas. It is the fourth state of matter and constitutes more than 99% of the universe. It consists of electrons, ions and neutrals which are in fundamental and excited states. From a macroscopic point of view, plasma is electrically neutral. However, it contains free charge carriers and is electrically conductive.

A plasma is created by applying energy to a gas in order to reorganize the electronic structure of the species (atoms, molecules) and to produce excited species and ions. This energy can be thermal, or carried by either an electric current or electromagnetic radiations.

The atmospheric plasmas described in this paper are generated from electrical energy. The electric field transmits energy to the gas electrons (which are the most mobile charged species). This electronic energy is then transmitted to the neutral species by collisions. These collisions follow probabilistic laws and can be divided in:

- Elastic collisions: they do not change the internal energy of the neutral species but slightly rise their kinetic energy.
- Inelastic collisions: when electronic energy is high enough, the collisions modify the electronic structure of the neutral species. It results in the creation of excited species or ions if the collisions are energetic enough.

Most of the excited species have a very short lifetime and they get to ground state by emitting a photon. The "metastable species" are also excited states but with a long lifetime because their decay by emission of radiation is hampered as there are no allowed transitions

departing from the respective state: decay can only take place by energy transfers through collisions.

2.1.1 *Plasmas classification*

Depending on the type of energy supply and the amounts of energy transferred to the plasma, the properties of the plasma change, in terms of electronic density or temperature. These two parameters distinguish plasmas into different categories. The atmospheric plasma sources described here are supposed to be positioned near the glow discharges and the arcs.

In this classification, a distinction can be made between:

- Local thermodynamic (or thermal) equilibrium plasmas (LTE).
- Non-local thermodynamic equilibrium plasmas (non-LTE).

LTE plasmas

LTE plasma requires that transitions and chemical reactions are governed by collisions and not by radiative processes.

Moreover, collision phenomena have to be micro-reversible. It means that each kind of collision must be balanced by its inverse (excitation/deexcitation; ionization/recombination; kinetic balance).

Moreover LTE requires that local gradients of plasma properties (temperature, density, thermal conductivity) are low enough to let a particle in the plasma reach the equilibrium: diffusion time must be similar or higher than the time the particle need to reach the equilibrium [5]. For LTE plasma, the heavy particles temperature is closed to the electrons temperature (ex: fusion plasmas).

According to the Griem criterion [6], an optically thin homogeneous plasma is LTE if the electron density fulfills:

$$n_e = 9 \cdot 10^{23} \left(\frac{E_{21}}{E_{H^+}} \right)^3 \left(\frac{kT}{E_{H^+}} \right) (m^{-3}) \quad (2.1)$$

where

- E_{21} represents the energy gap between the ground state and the first excited level.
- $E_{H^+}=13.58$ eV is the ionization energy of the hydrogen atom.
- T is the plasma temperature.

This criterion shows the strong link that exists between the required electron density for LTE and the energy of the first excited state.

Those rules for LTE are very strict. Thus most of the plasmas deviate from LTE,

especially all types of low density plasma in laboratories.

Non-LTE plasmas

Departure from Boltzmann distribution for the density of excited atoms can explain the deviation from LTE. Indeed, for low-lying levels, the electron-induced de-excitation rate of the atom is generally lower than the corresponding electron-induced excitation rate because of a significant radiative de-excitation rate. Another deviation from LTE is induced by the mass difference between electrons and heavy particles. Electrons move very fast whereas heavy particles can be considered static: electrons are thus likely to govern collisions and transitions phenomena. Deviations from LTE are also due to strong gradients in the plasma and the associated diffusion effects.

It has been shown that the LTE distribution can be partial. For example, LTE can be verified for the levels close to ionization threshold [7] (e.g., 5p levels and higher, in argon plasma): such plasmas are pLTE (partial LTE).

The non-LTE plasmas can be described by a two temperature model: an electron temperature (T_e) and a heavy particle temperature (T_h). Regarding the huge mass difference between electrons and heavy particles, the plasma temperature (or gas temperature) is fixed by T_h . The higher the departure from LTE, the higher the difference between T_e and T_h is.

Atmospheric pressure plasmas

Figure 2.1 shows the influence of the pressure on the transition from a glow discharge

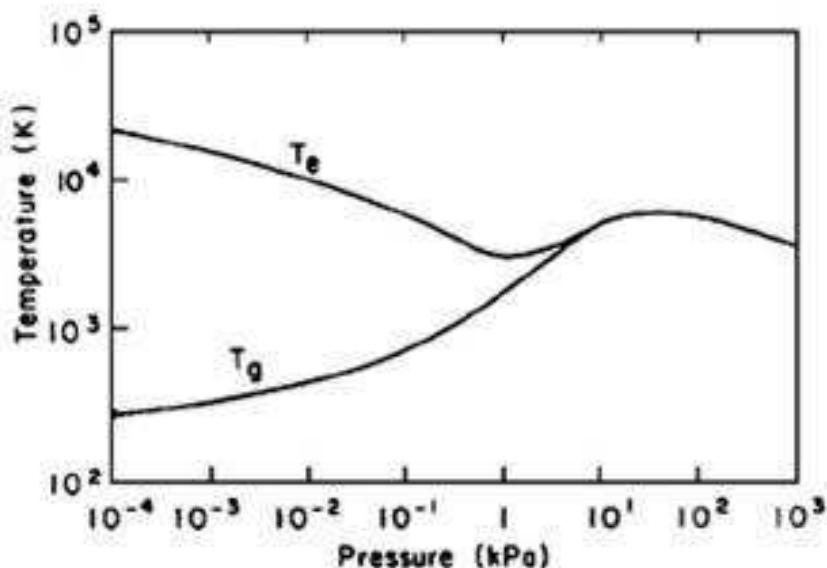


Figure 2.1: Evolution of the plasma temperature (electrons and heavy particles) with the pressure in a mercury plasma arc.

($T_e > T_h$) to an arc discharge. Low pressure plasmas (10^4 to 10^2 kPa) are non-LTE. Heavy particles temperature is lower than the electronic one. The inelastic collisions between electrons and heavy particles are excitative or ionizing. These collisions do not rise the

heavy particles temperature.

When the pressure becomes higher, collisions intensify. They induce both plasma chemistry (by inelastic collisions) and heavy particles heating (by elastic collisions). The difference between T_e and T_h is reduced: plasma state becomes closer to LTE but does not reach it. The significant gradient of properties in plasma restricts a particle, moving in the discharge, achieving equilibrium.

The density of the feeding power influences a lot the plasma state (LTE or not). On the whole, a high power density induces LTE plasmas (e.g. arc plasmas) whereas non-LTE plasmas are favored by either a low density of feeding power or a pulsed power supply. In this latter case, the short pulse duration prevents the equilibrium state from establishing.

Finally, it is important to note that an atmospheric plasma jet can be divided in two zones:

- a central zone or plasma core which is LTE.
- a peripheral zone which is non-LTE. In this plume, heavy particles temperature is much lower than electrons one.

Indeed, for a free-burning argon arc [6], operating conditions (a pressure of 300 kPa, currents of 300 to 400 A) are necessary to reach a LTE state in the central portion. These conditions lead to an electron density of 10^{24} m^{-3} in the center. Departures from LTE occur in the outer regions of such arcs where the electron density decreases below 10^{24} m^{-3} .

Thus, the local thermodynamic equilibrium is a primordial notion since it induces the temperature of the plasma. It strongly depends on the kind of plasma source and is determining for its applications.

2.1.2 Overview of various atmospheric plasma sources

The excitation frequency is important since it influences the behavior of the electrons and the ions.

The atmospheric plasma sources can be classified regarding their excitation mode. Three groups are then highlighted:

- the DC (direct current) and low frequency discharges;
- the plasmas which are ignited by radio frequency waves;
- the microwave discharges.

Examples of various atmospheric plasma sources

✓ *Corona discharge* [7] is a non-LTE discharge with low current density. The device consists of a cathode-wire and an anode (the treated material), the DC power supply is

pulsed. The plasma creates a lighting crown around the wire: that is why this discharge is called "Corona".

When a negative high voltage is applied to the wire, the discharge is a negative corona.

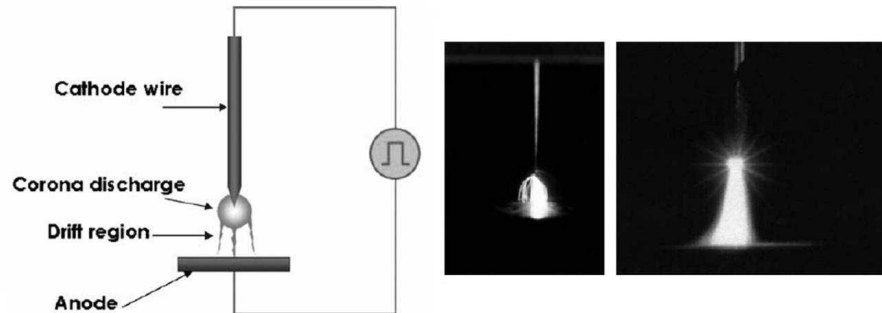


Figure 2.2: Principle of a Corona discharge and a hollow needle to plate discharge (left: positive needle, right: negative needle).

The positive ions are accelerated towards the wire where secondary electrons are emitted and accelerated into the plasma: this moving front of high-energy (about 10 eV) electrons followed by a tail of lower energy electrons (about 1 eV) is called a streamer.

Inelastic collisions occur between these high-energy electrons and heavy particles and induce the formation of chemically reactive species.

The pulses duration is shorter than the time necessary for the arc creation: when each pulse ends, the discharge extinguishes before it becomes too conductive. The transition into spark is then avoided. The current discharge is very low: 10^{-10} to 10^{-5} A. A positive corona also exists: the positive polarized wire acts as the anode.

As the plasma volume is very small, the main corona drawback regarding surfaces treatments is the thin size of the treated surface. To increase the size of the surface treatment, the cathode wire can be replaced by a planer electrode which is parallel to the treated surface: this system generates micro-arcs (streamers) that are perpendicular to the gap between the electrodes. The streamers always initiate at the same place (default on the surface) causing a non-homogeneous treatment on the material surface. To avoid this problem, a dielectric barrier discharge was developed.

✓ *Dielectric barrier discharge* (DBD) device (see figure 2.3) consists of two plane-parallel metal electrodes: at least one of these electrodes is covered by a dielectric layer. To ensure stable plasma operation, the gap which separates the electrodes is limited to a few millimeters wide. Plasma gas flows in the gap. The discharge is ignited by means of a sinusoidal or pulsed power source. Depending on the working gas composition, the voltage and frequency excitation, the discharge can be either filamentary or glow. A filamentary discharge is formed by micro-discharges or streamers that develop statistically on the dielectric layer surface. The use of helium as plasma gas seems to favor a glow discharge (high energetic He metastable species, Penning effect).

The dielectric layer plays an important part by:

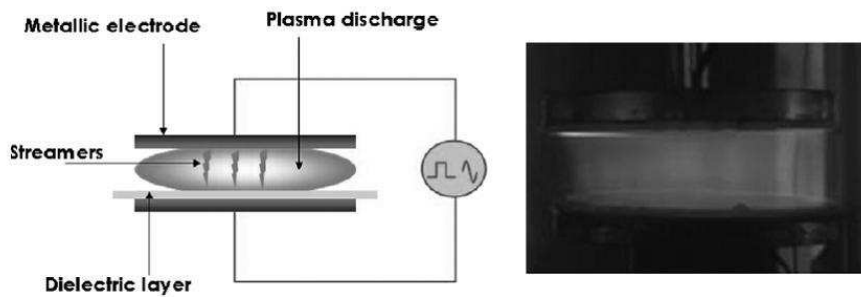


Figure 2.3: Principle of dielectric barrier discharge (picture: a non equilibrium diffuse plasma at atmospheric pressure).

- limiting the discharge current and avoiding the arc transition that enables to work with a continuous or pulsed mode.
- distributing randomly streamers on the electrode surface and ensuring a homogeneous treatment. The streamer creation is due to the electrons accumulation on the dielectric layer.

The described DBD device is the most common one and other systems have been developed:

- a DBD with a brush-style cathode that consists of 25 fine stainless wires. This process is convenient for nonconductive sample treatment,
- a system with a special designed cathode which can be applied to metallic and dielectric surface treatment,
- a DBD with spiral electrodes that are used for coating in the tube interior,
- a device where the dielectric layer consists of capillary dielectrics or a disc of glass beads.

✓ *A few atmospheric pressure plasma torches*

1) The arc plasma torches are fed by a DC power supply. They can be divided into two categories: current-carrying arc and transferred arc (see figure 2.4).

They both consist of:

- a cathode where electrons are emitted;
- a plasma gas injection system; and
- a nozzle which confines the plasma.

In a current-carrying arc torch, the nozzle which is positively polarized is the anode. In the case of a transferred arc torch, the treated material is the anode whereas the nozzle is at a floating potential.

The arc is ignited between the cathode and the anode and ionizes the plasma gas. The plasma temperature varies from 8 000 K (plasma envelop) to 15 000 K (plasma core)

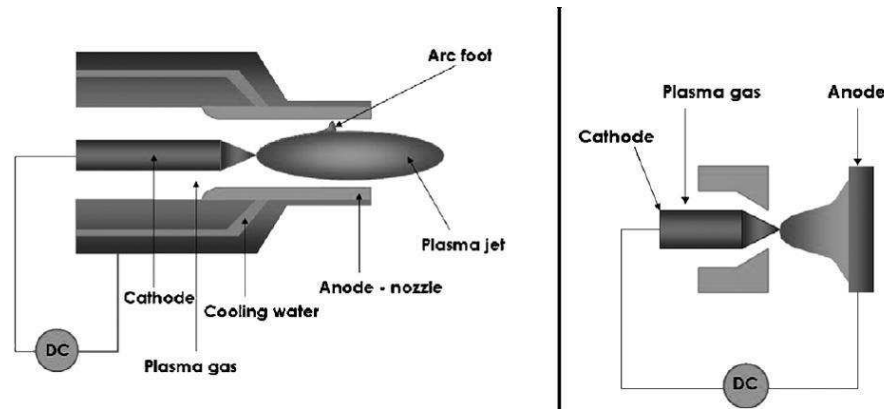


Figure 2.4: Principle of arc plasma torches (left: current-carrying arc; right: transferred arc).

which enables high temperature applications (use of the thermal effect of the plasma). An arc plasma is a very conductive media ($I = 50\text{-}600\text{ A}$). The gas is highly ionized and the electronic density is about 3.1023 m^{-3} .

2) Regarding their structure, the RF sources can work with a high or low power supply. It influences the properties of the plasma and thus its potential applications.

The impedance matching can be either inductive (high powered discharges) or capacitive.

The inductive discharges have been known for a long while. The RF torch is simply designed (see figure 2.5). The plasma is initiated and maintained by an RF fed helical coil.

The current that flows in the RF coil induces a time varying magnetic field nearby the

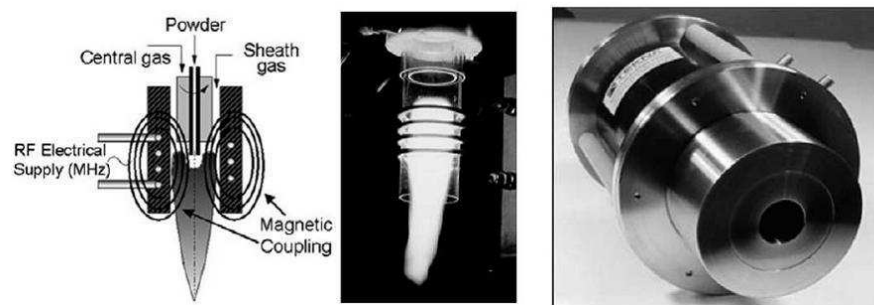


Figure 2.5: RF plasma torch.

plasma zone. The resulting electric ring field (see Faraday law) accelerates the electrons and thus maintains the discharge. The frequency of the generated plasma is higher than 1 MHz. This frequency level implies that electrons follow the electric field oscillations and neither ions nor electrons can reach the torch wall. This lack of contact between the plasma and the wall reduces the pollution of plasma and torch walls which enables to work with different gases: inert, reductive, oxidant, nitriding gas.

The plasma is enclosed in a ceramic tube (quartz, silicon nitride) that is cooled by air

or water, depending on the working power. The inductive torches work in a wide power range: 20 kW - 1000 kW, with a gas flow rate of 10 - 200 slm. A higher working power is accompanied with lower torch diameter and lower plasma frequency.

3) The cold plasma torch lies between the DBD and APPJ structures. The device is shown in figure 2.6 and its properties are. The RF electrode is a stainless-steel needle. A quartz tubing is inserted between the cathode and anode to ensure both plasma stability and homogeneity. The plasma gas flows into the gap between the cathode and the dielectric tube.

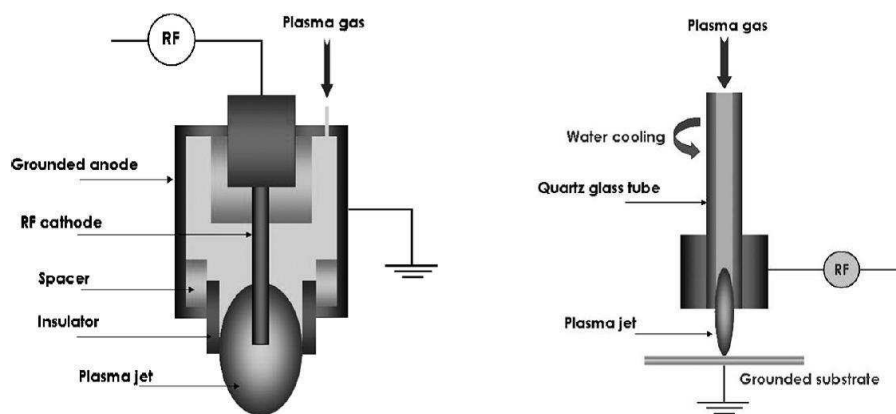


Figure 2.6: Left: cold plasma torch design. Right: barrier torch design.

4) A barrier torch (figure 2.6) which is similar to the RF pencil was also developed in Czech Republic by Hubie'ka et al. (Academy of Sciences, Prague). A quartz tube is inserted into the RF hollow electrode. The working gas is injected inside the dielectric tube. The dielectric layer stabilizes the discharge and limits the electrode heating. The discharge remains stable in the case of a multi-nozzle torch-barrier device. A larger surface zone can be treated.

✓ *The atmospheric pressure plasma jet (APPJ)* is a small ($L < 20$ cm) RF plasma torch that works at low power. It was developed by J.Y. Jeong et al. (University of California, Los Angeles) in collaboration with J. Park et al. (Los Alamos National Laboratory [7]).

This system (see Fig. 16) consists of two concentric electrodes through which the working gas flows. By applying RF power to the inner electrode at a voltage between 100 and 150 V, the gas discharge is ignited. The ionized gas exits through a nozzle since the gas velocity is about 12 m s^{-1} . The low injected power enables the torch to produce a stable discharge and avoids the arc transition.

The same research team designed a rectangular version of the APPJ. This source produces a volumetric and homogeneous discharge in a 1.6 mm wide gap between two planar

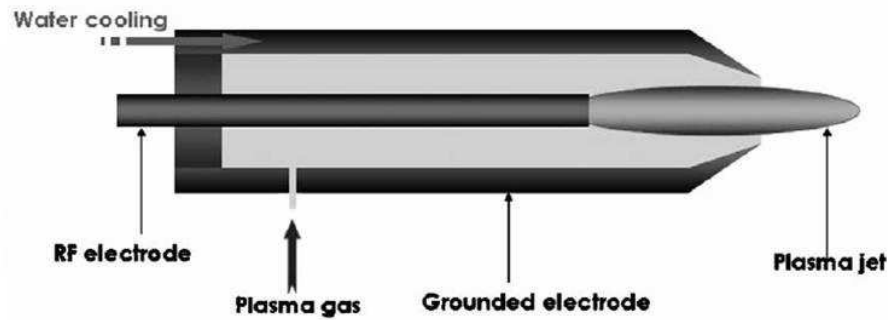


Figure 2.7: APPJ design.

aluminum electrodes. Both electrodes are perforated to let the plasma gas flow through them. The upper electrode is connected to the RF power supply while the lower electrode is grounded. It has been recently applied to the deposition of hydrogenated amorphous silicon with silane added downstream of the hydrogen-helium plasma.

2.2 Examples of industrial applications

2.2.1 Textile

In light of the disadvantages of low-pressure plasma systems, there has been increasing interest in atmospheric pressure plasma systems and applications in the textile industry [8]. The only available atmospheric pressure plasmas for textile industrial applications are glow discharge systems.

The three main glow discharges at atmospheric pressure are corona, dielectric barrier discharges (DBD) and atmospheric pressure glow discharge (APGD).

By accelerating the electric field, the lighter particles (electrons) achieve more kinetic energy than heavier ions and neutral gas particles. High-energy electrons induce collisions and release their kinetic energies to the surroundings, and then the plasma system reaches thermal equilibrium. In order to avoid thermal relaxation at atmospheric pressure, a largely inhomogeneous electric field is required. When sufficient voltages are supplied to accelerate electrons in the inhomogeneous electric field on one of the electrodes, a sharp needlepoint, a localized plasma (corona discharge) can be generated. An alternative way to prevent thermal relaxation at atmospheric pressure is to introduce a changing current frequency into a discharge. At low and high frequency, a discharge is initiated each time between the parallel electrodes. This discharge, found in DBD, could be generated under atmospheric pressure but would not remain uniform on the whole electrode area. Very narrow filaments are seen between electrodes in DBD.

Corona Systems for Textile Applications

Corona systems have been studied for availability in the textile industry because they can be operated in atmospheric pressure. Although many corona systems are utilized for continuous processing for mass production with high speed, some examples are presented in this paper. One of the early studies discussed is the improvement of shrink resistance for wool and mohair top. These results were obtained by using a continuous corona system, which was able to pass through substrates between parallel Pyrex electrodes as shown in Figure 4. This pilot scale corona device was available to not only make high-speed production of wool and mohair top, but also improve shrink-resistance and spinnability.

For another example, Abbot [9] showed the enhancement of cotton sliver cohesiveness

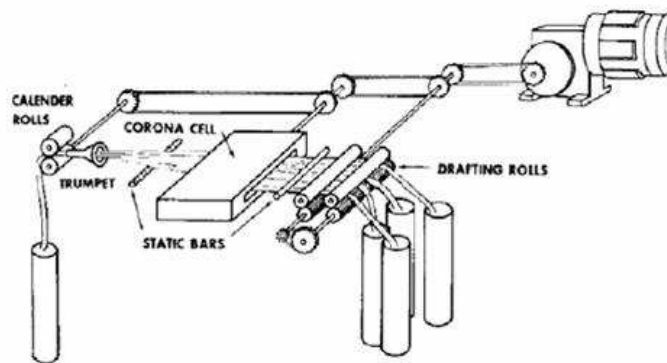


Figure 2.8: A schematic diagram of continuous corona discharge system for wool and mohair.

using the corona systems with a cotton sliver passing between the large and small corona rollers. Softal Electronic GmbH (Hamburg, Germany) [10] developed a continuous corona system for film surface modification. This system was designed for the roll-to-roll process, applying to adhesion, coating, printability and deposition. Sherman Treaters Co. (Oxon, UK) [8] designed a continuous corona system for surface modification of polypropylene tow following melting spinning process (figure 2.9). These results showed improvement of antistatic, friction and wettability of the treated fibers, and could reduce the quantity of spinning finish added resulting in cost-saving, environmental issues and fiber performance.

Atmospheric Pressure Glow Discharge (APGD) for Textile Applications

The foundation of a stable and homogeneous plasma under atmospheric pressure was reported in 1998 [11]. This stable and homogeneous discharge required the following conditions:

- 1) Helium was used as dilute gas,
- 2) Heat resistance insulating plate was set on the lower electrode plate while upper electrode was a brush style, and
- 3) Power supply frequencies were 3,000 Hz and Radio-frequency (13.56 MHz).

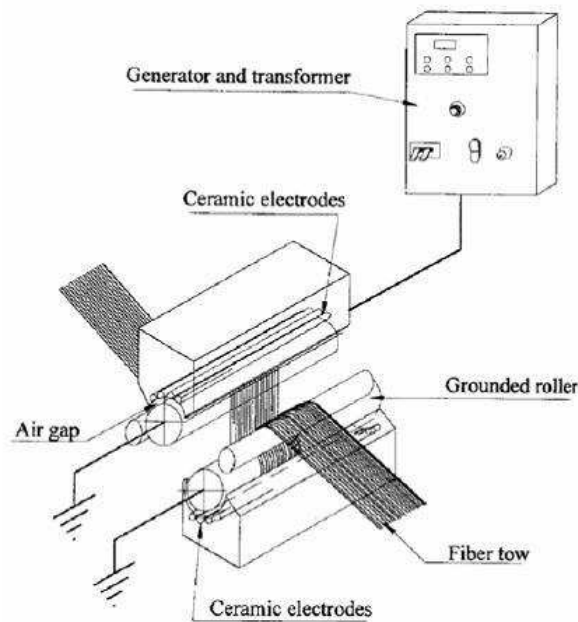


Figure 2.9: A schematic diagram of continuous corona system for Polypropylene Fiber Tow designed by Sherman Treaters [8].

However, this discharge could be transformed into thermal plasma such as arc discharge when strict plasma conditions were not applied. Fluorination of poly (ethylene terephthalate) (PET) film was successful compared to the results in vacuum plasma using optical emission spectroscopy. Roth and co-workers developed the one atmospheric glow discharge plasma reactor, called one atmosphere uniform glow discharge plasma (OAUGDP), and applied plasma treatment to textile materials [12] for surface modification and sterilization [13]. This reactor has two parallel electrodes covered by an insulating coating and can generate uniform plasma in helium according to Kanazawa's model [11].

Another independent development of APGD was carried out at North Carolina State University, the parallel plate atmospheric plasma device for industry (PALADIN), designed specifically for the industrial applications [14].

Atmospheric pressure plasma systems are suitable for textile industrial applications, which involve mass production at high speeds, because it is possible to carry out continuous processing without size limitation. Recently, even though atmospheric pressure plasma systems were developed in Japan and the United States, Dow Corning Plasma Solutions is the only available APGD machine manufacturer for textile applications in the world. A model of APGD, AP-100 (width 100 cm, but width of machine is variable depending on textile process conditions), is able to generate a stable and uniform glow discharge and leads to continuous processing at a maximum speed of 60 m/min.

Dow Corning Plasma Solutions has supplied APGD plasma systems to several production lines in Europe. One of them, installed at Institute of Fiber and Polymer Tech-

nology Research (IFP, Sweden), is applied to adhesion enhancement of polymer coatings (Almedahl AB, Sweden), surface modification of automobile textiles (Borgstena Textile Sweden AB, Sweden), increasing hydrophobicity of cellulose based materials, and improvement of adhesion of polymer materials (SCA Hygiene Products AB, Sweden). In German, Kirchhoff GmbH and Co. has been applying APGD plasma system to anti-shrinkage finishing. The same APGD system at Polisilk S.A. in Spain is being used to improve binding properties of polypropylene-based coating. In addition, Plasma Ireland supplied another APGD system to Scapa Group in England for printing applications.

Plasma Applications to Textile Processing

Wettability Enhancement

The wettability enhancement of polymeric surfaces can be obtained easily by plasma treatment in oxygen containing gas. However, after exposure to air, the wettability is not durable due to the ageing process. For the textile applications of wettability enhancement, increased durability has been obtained using plasma graft polymerization techniques. The monomers used in plasma graft polymerization for wettability enhancement are acrylic acid, nitro compounds, 2-hydroxyethyl methacrylate (HEMA), methyl methacrylate (MMA), acrylamide (AAM) and acrylonitrile [8].

In 1971, the first commercial application of plasma graft polymerization for wettability enhancement on fabrics was conducted by Bradley [15]. After surface functionalization by argon plasma for PET fabrics, the acrylic acid monomer was introduced into vacuum chamber leading to uniform grafting polymerization. This technique could render PET fabrics as wettable as cotton and improve moisture retention and washing durability. In addition, handle properties of fabrics were improved without alteration bulk properties. Cotton fabrics treated by this technique showed better hand properties obtained.

There is another and specially developed activation process that can be used to make the surface hydrophilic (figure 2.10). This permanently hydrophilic character is used to give woven, and non woven textiles the capability to be used as blood filter or filtering membranes for specific applications. Applications are micro filtration systems based on these textiles or capillaries: blood filters, dialysis filter systems etc.

Water Repellent Finishing

Fluorocarbon, hydrocarbon and mixtures of fluorocarbon and hydrocarbon gases have been used to increase hydrophobicity of polymer substrates in plasma. Compared to oxygen and air plasma treatment, fluorocarbon and mixtures of fluorocarbon and hydrocarbon gas plasma showed higher durability in air exposure [8].

Iriyama et al. [16] studied the water-repellency of nylon fabrics treated in fluorocarbon plasmas (CF_4 , C_2F_4 , C_3F_6 and C_6F_{14}). The durability of water-repellency after 30 min. washing was better in fabrics treated with saturated fluorocarbon plasmas than unsaturated. The saturated fluorocarbon plasma introduced longer chains of polymer on fabric

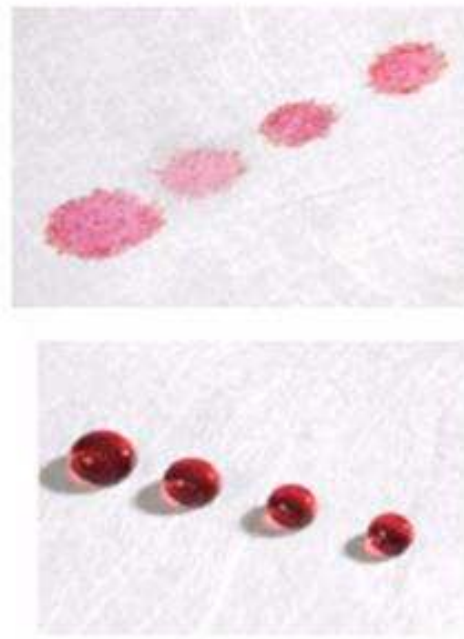


Figure 2.10: *Hydrophilic treatment of blood filters, capillaries (upper photograph): another and specially developed activation process can be used to make the surface hydrophilic. This permanently hydrophilic character is used to give woven, and non woven textiles the capability to be used as blood filter or filtering membranes for specific applications. Applications are micro filtration systems based on these textiles or capillaries: blood filters, dialysis filter systems etc. Hydrophobic treatment of non woven PP (bottom photograph): by using semi-continuous textile treaters it is possible to plasma polymerize the surface of non woven and other textiles so that they become hydrophobic of nature. A lot of industrial users are looking to replace their conventional techniques or improve the final result by using plasma technology. Applications are oleophobic or hydrophobic treatment of paper, tissues and filter elements.*

surface (figure 2.10), leading to better hydrophobicity and durability. Wang et al. [17] found similar results from plasma treatment on PET film with mixtures of fluorocarbon and methane.

McCord et al. [18] found that the fluorocarbon functional group, $-CF_3$, played an important role in increasing water-repellency.

Anti-shrinkage Finishing

Anti-shrinkage finishing using plasma treatment is the first successful commercialized technique for the textile industry. The first attempt at anti-shrinkage finishing was a corona treatment for wool fabrics [8]. Wool garments treated by corona showed better shrink resistance and stability than untreated. Thorsen et al. [19] suggested that corona treatment could be applied to mass production of wool fabric to improve shrink resistance. Compared to corona treatment, the efficiency of anti-shrinkage in plasma treatment shows better effect. Recently, low-pressure plasma and corona are available for anti-shrinkage finishing in textile industry. Plasma treatment is considered an environmentally friendly alternative to the conventional anti-shrinkage finishing, wool chlorination.

Regardless, further studies are still needed to apply plasma treatment to industrial production for anti-shrinkage finishing as well as enzymatic treatment, which is another possible environmentally friendly method for anti-shrinkage finishing.

Oxygen was known as the most effective gas for shrink proofing of wool fabrics made from plasma-treated yarns [8].

Desizing

The application of size to warp yarns before weaving plays an important role in enhancement of weaving efficiency due to an increase of yarn strength and reduction of yarn hairiness. Also, it is important to remove size after weaving for further processes, dyeing and finishing. The conventional desizing process is conducted by washing in hot water bath.

Regardless of high temperature, complete removal of size on fabrics is impossible due to redeposited sizes on yarns during the desizing process, resulting in poor bleaching, dyeing and printing. Moreover, the desizing waste is a major concern of pollution world-wide, even though a recycling technique is available.

Plasma desizing was performed as a novel technique to solve the environmental problem of desizing [8]. The plasma desizing process consisted of two steps: gas plasma treatment on the sized fabric and washing in solution. Compared to hydrogen peroxide desizing, plasma treatment plus cold-water washing showed better size removal on cotton fabrics. Oxygen plasma was more effective in desizing than either air or nitrogen. Two possible plasma effects are involved in the plasma desizing. First one is gas vaporization of sizes by the etching effect of plasma.

The second one is hydrophilic functionalization of size molecules, possible in conjunction with either chain scission or cross-linking. The increase in hydrophilic groups may

lead to higher solubility in wash solution.

Flame Retardant Finishing

Flame retardant finishing of textiles has been accomplished via plasma treatment. As one of initial studies for flame retardant finishing on textiles, researchers studied flame retardant finishing on natural and synthetic fabrics. The fabrics pre-absorbed with phosphorus and halogen containing monomers were exposed to nitrogen low-pressure plasma, leading to graft polymerization on fabric surface. The graft polymerization by plasma with phosphorus and halogen containing monomers improved the flame retardant properties of fabrics.

In addition, it was proposed that plasma application of flame retardant finishing could have economical and environmental advantages compared to conventional wet-chemical finishing processes. For flame retardant finishing for cotton fabrics, cotton fabrics treated by argon plasma with THPOH/NH₃ and H₂O₂ washing were durable to 50 launderings and launderings with chlorine bleaching.

Adhesion Enhancement

Most of composite materials, including UHMPE (ultrahigh modulus polyethylene), PPTA (poly(p-phenylene terephthalate) and carbon fibers, have excellent mechanical properties. However, chemical inertness and smoothness of their surfaces can be a serious problem to apply to resin matrix for composite applications. Compared to conventional wet chemical surface modification, plasma techniques can overcome the disadvantages of high performance fibers easily and improve adhesion to resin matrix without altering physical properties.

Ultrahigh-modulus polyethylene (UHMPE) fibers such as Spectra. fibers do not form strong bonds with most commercially available matrix materials due to their inert chemical structure. Low-pressure plasma treatments have been shown to greatly enhance the bonding between UHMPE fiber and resin matrices such as epoxy and vinyl ester resins [20].

The plasma treatment created not only micro-roughness on the surface of UHMPE fibers, resulting in a better mechanical interlocking of the fiber surface to resin matrix, but also functional groups, leading to chemical interfacial bonding between the fiber and matrix.

Dyeability Enhancement

Dyeing in textile industry requires the development of environmentally friendly and economic processes due to pollution and economic limitations. Plasma techniques have been studied to replace or aid the conventional wet dyeing process. The initial approach of plasma was corona treatment.

As an example, Wakida et al. [21] showed the possibilities of atmospheric pressure plasma for wool fabric dyeing applications. The atmospheric pressure plasma treatment

with a mixture of helium and argon was very effective on the reduction of half-dyeing time and an increase of dye exhaustion with acid dyes.

Sterilization

Sterilization processes are designed to destroy viable microorganisms before biomaterial contact with living organisms. In general, either a physical or chemical process or both are carried out sterilization. The conventional sterilization methods including heat, radiation, and chemical treatment can terminate the microorganisms [8]. Heat treatment is an easy method but bacteria with a pore could survive at high temperature and under some conditions. Additionally, heat treatment is not acceptable to low-melting polymer materials and it needs a relatively long period treat time. Ethylene oxide (ETO) is used as a chemical treatment to sterilize many polymeric medical products. However, ETO is not only a highly toxic gas causing cancer but easily absorbed in plastic materials. Gamma radiation and X-ray can exterminate bacteria or viruses by breaking bonds inside the bacteria cells and virus capsides. However, some of microorganisms resist radiation, and radiation causes undesirable changes of substrate.

Because the power density of atmospheric plasma is not high, it does not alter the bulk properties of substrates where bacteria and viruses live. Also, the successful design of a remote exposure reactor can eliminate many constraints of workpiece size and shape.

Recently, the atmospheric pressure plasma has been investigated as novel sterilization technique [13]. One of successful designs is one atmosphere uniform glow discharge plasma (OAUGDP, University of Tennessee, Knoxville (UTK)).

Koulik et al. [22] proposed the mechanism of sterilization under atmospheric pressure plasma as following;

- 1) Plasmochemical reaction: oxidation and etching,
- 2) Electron bombardment,
- 3) UV radiation,
- 4) Surface ablation and
- 5) Chemical reaction after plasma treatment.

As an italian living reality the University of Milano-Bicocca, together with the Regione Lombardia and the Fondazione Cariplo, supported the creation of a Centre of Excellence on Plasma Applications as depicted in figure 2.11.

Mainly they work on:

- Plasma Processing for polymers, gas sterilization and VOC abatements; coating, plasma spray, dusty plasmas;
- Plasma Processing for Energy: hydrogen production and waste treatments by plasma, plasma Fuel Converter (PFC) for producing hydrogen rich mixtures, plasma torch for waste treatments;
- Plasma processing for biomedical applications







Technology on atmospheric plasma: A reality for the textile field

A new plasma technology highly innovative in the field of superficial treatments of the materials, it is based on a DBD electric discharge. (Dielectric barrier discharge)
Radicals, active chemical species and loaded species are produced and with them it is possible to realize processes of non-conventional superficial modification.



NANOTECHNOLOGY

The modifications applied to the surface are on nanometre scale at room temperature.

THE PROCESSES

The superficial modifications take place thanks to the high plasma reactivity and processes trigger.

- Physical type (bombing of the surface)
- Chemical type (reactions with radicals).



- Reaction of atoms insertion or complete chemical groups (grafting)
- Generation of free radicals on the surface. (Attivazione).
- Polymers deposition in a gaseous phase as thin layer adherent to the surface (film deposition)
- Superficial ablation of the material (etching).

ADVANTAGES

INNOVATION:

- It generates innovative materials and new surface properties.
- It does not modify the bulk property of the material.

ENVIRONMENT:

- Negligible quantity of chemicals.
- Dry process, which does not require solvents or chemicals dangerous for the environment.
- The DBD technology with respect to the plasma common technologies operates at ATMOSPHERIC PRESSURE
- Production processes in continuous way.
- Process times are highly reduced.
- All disadvantages due to the preparation of vacuum plants are avoided.
- It is not necessary to use seal devices.



ENERGY SAVING AND A LOWER ENVIRONMENTAL IMPACT.

THE APPLICATIONS	THE FABRIC
<ul style="list-style-type: none"> Increase of wettability. Increase of hydrophilicity Water-repellent and oil-repellent surfaces achieved. Biocompatibility (antibacterial properties of adhesion and affinity to proteins and other bio molecules). Dyeable (increase of dyeing speed). Print (increase of absorbed colour quantity by the textile fibres). Adhesion (increase of spreading adhesion with specific compounds.) 	<p>It is applied to fabrics and yarns of natural and artificial fibres without modifying its bulk properties:</p> <ul style="list-style-type: none"> The organoleptic properties and the transpiration are unchanged. Fabrics with multifunctional properties can be obtained. They can be applied to all textile-working phases from the fibre until fabric finishing process. They can be easily introduced into the productive processes <p>The materials that can be functionalised are: Polypropylene, polyethylene polyester, nylon, natural textile fibres, etc....</p> <ul style="list-style-type: none"> Fabrics for clothing. Fabrics for furnishings Technical fabrics (filtration, medical, pharmaceutical). Non-woven fabrics.

THE PROTOTYPE

Realised for the project "Metadistretti per l'eccellenza Lombarda", with "ARIOLI s.p.a.", textile machinery enterprise, as leader company, together with the research institutes "Stazione Sperimentale per la Seta" and "Plasma Prometeo" of "Università degli Studi - Milano-Bicocca"

- It is based on DBD discharges.
- It operates under atmospheric pressure with air or inert gas and several gas mixtures.
- It produces plasma between two or more electrodes in which the fabric runs.
- Different speeds (1-60 m/min).
- Treatment on one or both fabric sides.
- Fabric width up to 400 cm.

At the moment: excellent results with water repellence and hydrophilic. Research projects for the development of other processes of textile interest are in progress..

With the realized prototype, it is therefore possible to carry on experiments and to realize applications at industrial level on various technical and traditional textile products for furnishing and clothing use.

CLAUDIA RICCARDI, PlasmaPrometeo, Università degli Studi di Milano-Bicocca
MARIA ROSARIA MASSAFRA, Stazione Sperimentale per la Seta
STEFANO FORT, Arioli s.p.a. www.arioli.it

Figure 2.11: To promote the Research and the Technological Transfer in the field of Plasma Applications, the University of Milano-Bicocca, together with the Regione Lombardia and the Fondazione Cariplo, supported the creation of a Centre of Excellence on Plasma Applications. The Centre of Excellence PLASMAPROMETEO was established on February 12th 2004 on the basis of an agreement between the University of Milano-Bicocca and the Regione Lombardia. The aims of the Centre is to promote Technological Transfer and training to Small Medium Enterprises. (<http://www.plasmaprometeo.unimib.it/history.php>)

- Plasma Processing for Cultural Heritage
- Technological Transfer to Industries
- Development of semi-industrial prototypes
- Formation and Technical assistance
- Technical and economical evaluation for industrialization of new plasma technologies

2.2.2 *Bottles and Displays*

Pretreatment with atmospheric pressure plasma is arousing ever more interest among users who require microscopically fine precleaning and high activation of surfaces prior to the painting process. Whether it is a light switch or mobile phone housing, display or perfume bottle manufacturers are putting ever more effort into improving their surface coating processes. This also requires action to optimize pretreatment.

Pretreatment processes range from ionization or flame treatment through wet chemical processes, power washing and use of primers right up to dusting with ostrich feathers. Despite the sometimes high investments made, the proportion of reject parts in production caused by painting over particles of dust is often well above 10 %.

Static charging of surfaces, tiny but still unacceptable remnants of fine dust in less accessible areas or environmental pollution are the most common problems in the aforementioned processes.

Plasma pretreatment brings about microscopically fine cleaning and high activation of the most varied surfaces and hence promotes optimum adhesion of paints and adhesives (figure 2.12). Moreover, plasma cleaning is more economical than conventional pretreatment methods while at the same time being very environmentally friendly.


The atmospheric pressure "Open-air" plasma process developed by Plasmatreat opened up new possibilities: by developing and employing plasma jets this state of matter, scarcely used hitherto in industry, has now been successfully used for the first time in production processes, even in-line.

The systems based on a jet principle operate at atmospheric pressure and with the aid of an electric arc ignited in the jet and the working gas, air, produce a plasma which flows at zero potential onto the surface of the product to be treated. It contains enough excited particles to produce selective effects on the surface.

The emergent beam of plasma's density is so high that operating speeds of 100 m/min are achievable. Heating of plastic surfaces during treatment typically amounts in this case to $\Delta T < 20^\circ\text{C}$.

In the process the surface is activated and adhesion is significantly improved. Due to the process of discharging on surfaces the plasma system affords cleaning effects which are superior to those of conventional systems. The decisive factor in this is the electrostatic discharge action of a free beam of plasma. This effect is reinforced by the high outflow rate of the plasma as a result of which loosely adhering particles are removed from the surface.



tantec 
www.tantec.com





PlasmaTEC Atmospheric Plasma Treatment

The purpose of surface treatment of polymer-based materials is to increase surface wettability through electrical discharge. The low surface energy of polymer-based substrates often leads to poor adhesion of inks, glues and coatings. To obtain optimum ad-

hesion, it is necessary to increase the surface energy of the substrate to just above that of the material to be applied. Surface treatment with Plasma results in improved surface adhesion properties.

Plasma technology offers innovative solutions to adhesion or wetting problems in many industries.

Component preparation is an important step prior to bonding, painting, gluing, printing or coating processes. Plasma treatment provides an economical solution for the effective activation of complex shaped component surfaces before further processing.

PlasmaTEC conforms with CE regulations and carries CE marking.

Advantages:

- Multiple Plasma Treating Heads can operate from a single generator.
- The PlasmaTEC and conventional Corona can work simultaneously from a single generator.
- A number of different nozzle tips are available for the effective treatment of a large variety of different parts.
- Potential free discharge.
- Suitable for high line-speed.
- No generator adjustments necessary.
- Easy to integrate into new or existing production lines.

electrical surface treatment



Figure 2.12: Tantec has been offering cutting-edge and environmentally-friendly Plasma and Corona surface treatment equipment for over thirty years. Tantec develops, manufactures and markets innovative equipment worldwide for Plasma and Corona surface treatment of plastic components. Atmospheric Plasma treating system provides an economical solution for the cleaning and activation of complex surfaces before further processing. Component preparation is an important step prior to bonding, painting, varnishing and coating processes.

The Openair system is characterized by a threefold effect. It activates the surface by selective oxidation processes, simultaneously discharges the surface and due to high speed air currents cleans off loosely adhering particles.

Some examples of applications are described below and depicted in figure 2.13.



Figure 2.13: *The mobile phone housing is cleaned by a rotating plasma jet prior to painting. Vehicle manufacturer has been using Openair plasma for pretreating plastic surfaces. Switches with laser-etched symbols, high-gloss decorative strips and covers, scratch resistant displays and glittering fascias, ventilator grilles or glove compartments even plastic parts in the interiors of automobiles can be pretreated using plasma.*

The mobile phone housing is cleaned by a rotating plasma jet prior to painting. The highest demands are imposed on the surfaces of mobile phone housings. The paint finish must be free of defects and its overall appearance must not be impaired by imperfections. Electrostatic adhesion of dust and particles transferred from the injection mould are the principal causes of this.

Suppliers to the mobile phone industry in South Korea and Finland have already responded positively. Here Plasmamatreat (<http://www.plasmamatreat.com/>) installed units for cleaning mobile phone housings. These provide extremely efficient cleaning in in-line processes. Immediately prior to painting, several rotating plasma generators very efficiently clean the plastic surfaces. The users were able to reduce the proportion of rejects from 12% to less than 5%.

For two years a vehicle manufacturer has been using Openair plasma for pretreating plastic surfaces. The high demand for vehicles having expensive multiple layers of paint caused bottlenecks in the curing ovens.

A vehicle part usually passes through many stations during the painting process. A typical plastic part is given a coat of primer adhesion promoter, up to eight coats of paint plus a clear coat. But ovens have limited capacity. Most manufacturers have only one paint line and one curing oven per factory. Thus, one part will travel through the same oven from four up to nine times. Any way a manufacturer can increase capacity without cost-intensive procurement of new equipment results in significant cost savings.

In the present example it is not possible to retain the same high quality appearance of surfaces while reducing the number of finishing coatings used. However, with the aid of the plasma treatment it was possible to dispense with the primer coating promoting adhesion. In this way the number of passes through the oven were reduced by 25% or conversely the capacity of the oven was significantly increased. In addition it was possible to eliminate the entire priming process and the high costs associated with it.

Switches with laser-etched symbols, high-gloss decorative strips and covers, scratch-resistant displays and glittering fascias, ventilator grilles or glove compartments even plastic parts in the interiors of automobiles are today provided with expensive coats of paint.

Here plasma technology can be used as a pretreatment process for these components both prior to bonding as well as prior to painting. Accordingly, to cite some examples, the process is used for vehicle parts made by BMW and Rolls Royce.

Pretreatment with atmospheric pressure plasma, however, is not just an issue for materials such as plastics or metals. It is also relevant to glass surfaces. Thus, the glass bottles for expensive perfumes are often painted, some even in multiple colors. The high-quality image of the bottles demands an immaculate surface and the most thorough cleaning of the material prior to the painting process. A German perfume bottle manufacturer is also profiting from the advantages afforded by plasma technology. It has been running a plasma pretreatment installation since last year.

Chapter 3

Radio-frequency atmospheric plasma cleaning applied to niobium resonant cavities

As already mentioned atmospheric pressure plasma treatment is an emerging, very versatile and inexpensive technique used in various surface process such as dry etching, chemical modification and surface wettability change. We decided to try to ignite a resonance atmospheric plasma into 1.5 GHz superconducting niobium cavities to perform a feasibility study. The second step has been the attempt to understand what really happens to the resonant structure internal surface. The most powerful tool consists in the atmospheric plasma treatment and fast rf characterization of 6 GHz small resonators.

3.1 *Experimental details*

The experimental set up, conceived to test atmospheric plasma treatments, consists essentially in the rf and cryogenic systems used to test the cavity quality. The only modification that has to be considered is the adding of a gas line.

3.1.1 *rf apparatus*

The rf apparatus we use has been already described elsewhere ([23, 24]), I just want to give the basic information to simplify the comprehension of the following sections.

Fundamental equations for rf test

During the rf tests on cold cavities the basic rf properties such as maximum accelerating gradient (E_{acc}), field emission onset, and quality factor Q_0 , as a function of E_{acc} are determined. These tests (that have to be performed at (or near) the *critical coupling*) are done inside a cryostat where the cavity is held vertically.

The critical variable for calculating the rf parameters of a superconducting cavity is the shunt impedance, which relates the stored energy to the effective accelerating gradient. It (together with the resonator geometry) is the quantity necessary for calculating the peak electric and magnetic fields for any given mode. In our case it is determined using the electromagnetic simulation tool called Superfish [25]. All the important parameters determined for 1.5, 1.3 and 6 GHz cavities are collected in tables 3.3 and 3.2 .

Symbol	Variable name	Units
r/Q	Geometric shunt impedance	Ω/m
G	Geometry factor	Ω
E	Electric field	V/m
L	Electrical length	m
ω_0	cavity frequency	s^{-1}
U	Stored energy name	J
R_s	Surface resistance	Ω
Tc	Critical temperature	K
P_{emit}	Emitted power	W
R	Shunt impedance	Ω
T	Operational temperature	K
R_{res}	Residual surface resistance	Ω
Q_0	Intrinsic quality factor	
Q_{cpl}	Fundamental Power coupler coupling factor	
Q_{pk}	Field probe coupling factor	
R_C	Coupling impedance	Ω/m
P_{diss}	Dissipated power	W
τ	Decay time	s
r	Shunt impedance per unit length	Ω/m

Table 3.1: Common variables when discussing rf cavities [26].

When a cavity mode oscillates with a resonant frequency ω_0 , a stored energy U and rf losses on the cavity walls, P_d , the quality factor can be defined as:

$$Q_0 = \frac{\omega_0 U}{P_d} \tag{3.1}$$

Q_0 is 2π times the stored energy divided by the energy consumed in one period. In the frequency domain the Q_0 can also be written as

$$Q_0 = \frac{\omega_0}{\Delta\omega_0} \tag{3.2}$$

where $\Delta\omega_0$ is the 3-dB band width. Unfortunately, the direct measurement of the 3-dB

band width of a superconducting cavity is practically impossible, because it can attain very small values as compared to the center frequency: some Hz or fractions of Hz out of thousands of Megahertz. This is much less than the resolution of any commercially available network or spectrum analyzer. For this reason, a time domain method must be used.

The cavity receives the rf power via an input cable and an input antenna (*coupler*, figure 3.1) from a power amplifier driven by a signal generator which is exactly locked onto the resonant frequency of the cavity mode ([23, 24]).

The transmitted power is extracted from the cavity by the output antenna (*pickup*

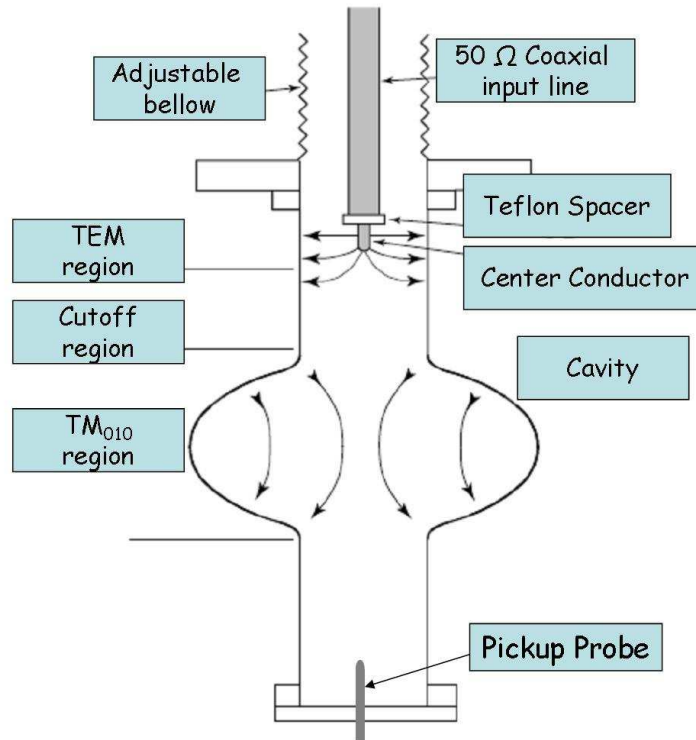


Figure 3.1: *Input coupler arrangement used to couple rf power into the cavity.*

probe) as depicted in figure 3.1.

All antennas are connected to calibrated *power meters* and it is possible to calculate the total power lost P_L with the following power balance:

$$P_L = P_d + P_{cpl} + P_{pk} \quad (3.3)$$

where P_d is the power dissipated in the cavity walls, P_{cpl} is the power leaking back out the fundamental power coupler and P_{pk} is the power transmitted out via the pick up antenna. This equation is valid for a cavity with no driving term that has a stored energy equal to U .

In this condition the so called "*Q loaded*" is introduced to take into account the reso-

nant circuit behavior when it is coupled with an external line:

$$Q_L = \frac{\omega_0 U}{P_L} \quad (3.4)$$

The quality factor, for each dissipated power, could be written as:

$$Q_0 = \frac{\omega_0 U}{P_d} \quad Q_{cpl} = \frac{\omega_0 U}{P_{cpl}} \quad Q_{pk} = \frac{\omega_0 U}{P_{pk}} \quad (3.5)$$

Those Q values are proportional to the number of cycles the system needs to dissipate all the energy on the considered transmission line. It's important to control if the dissipated power in the couplers is higher or lower than the power dissipated on the cavity walls.

It follows that:

$$\frac{1}{Q_L} = \frac{1}{Q_0} + \frac{1}{Q_{cpl}} + \frac{1}{Q_{pk}} \quad (3.6)$$

Each transmission line has its own external coupling factor β defined by:

$$\beta_x = \frac{Q_0}{Q_x} = \frac{P_x}{P_d} \quad (x = cpl, pk) \quad (3.7)$$

The transmission antenna should be sized in order to avoid perturbation of the cavity operation: this condition is reached when $\beta_{pk} \ll 1$. In this way the antenna pickups the bare minimum energy required for the measurement. Moreover it must be far enough from the coupler antenna to avoid the signal transmission without resonance inside the cavity (*no cross-talking*). On the other side, to be able to transfer all the input power to the cavity, the coupler should satisfy the condition $\beta_{cpl} = 1$. Thus it assures a perfect match between the system and the cavity electrical impedances (*coupling*). In other words, when $\beta_{cpl} = 1$ the input power equals the power dissipated on the cavity walls plus the small amount of power that goes out of the pickup port:

$$P_d = P_i - P_{ref} - P_{pk} \quad (3.8)$$

where P_i is the incident power, P_{ref} is the reflected power and one assumes that $P_{pk} \ll P_d$.

Impedance matching is essential otherwise a mismatch causes power to be reflected back to the source from the boundary between the high impedance and the low impedance. The reflection creates a standing wave, which leads to further power waste. The impedance matching device is the *antenna tuner*. When β is not equal to 1 (i. e. systems with a fixed input antenna or cavities when used to accelerate beam) the determination of the stored energy becomes more complex. More details on the calculation necessary for such cases are given in reference [26]. Fortunately, our system allows us to achieve critical coupling

prior to doing a decay measurement. This simplifies maths and allows us to make the assumptions described below.

When switching off the power supply, the cavity enters into a state of free decay, losing energy due to dissipation on the cavity walls and the power flowing through the input and the output antennas. During a free decay, the power lost corresponds to the variation with time of the stored energy, thus:

$$\frac{dU}{dt} = -P_L = -\frac{\omega_0 U}{Q_L} = -P_d - P_{cpl} - P_{pk} \quad (3.9)$$

the solution (assuming that Q_L is independent of U) is an exponential decay, with

$$U = U(0) \cdot e^{-\frac{t}{\tau}} \quad \tau = \frac{Q_L}{\omega_0} \quad (3.10)$$

The decay time constant τ is experimentally measured and it is used to calculate a value for the loaded-Q, Q_L . Then Q_L , P_i , P_{ref} , P_{pk} are used to calculate Q_0 . In fact when the cavity is critically coupled:

$$Q_0 = (1 + \beta_{cpl} + \beta_{pk})Q_L = 2Q_L = 2\omega_0\tau \quad (3.11)$$

$$Q_{pk} = \frac{2\omega_0\tau(P_i - P_{ref} - P_{pk})}{P_{pk}} \quad (3.12)$$

In summary, P_i , P_{ref} , P_{pk} and τ are sufficient to derive Q_L and Q_{pk} . The next step consists in the incident power increasing in order to raise the stored energy value U . Q_{pk} is a constant that is strictly dependent on the probe and cavity geometries. Thus, using Q_{pk} , Q_0 and E_{acc} can be evaluated:

$$Q_0 = \frac{Q_{pk}P_{pk}}{P_i - P_{ref} - P_{pk}} \quad (3.13)$$

The gradient may then be calculated as:

$$E_{acc} = \sqrt{Q_{pk}P_{pk} \frac{r/Q}{L^2}} \quad (3.14)$$

3.1.2 *Cryogenic infrastructure*

The basic information about the cryogenic infrastructures built to measure the rf properties of superconducting cavities are given. The idea is to place emphasis on the modifi-

Parameter		Tesla-type cavity		
		1.5 GHz	1.3 GHz	6.0 GHz
$2\pi f_0$	frequency (Hz)	$9.425 \cdot 10^9$	$8.168 \cdot 10^9$	$3.77 \cdot 10^{10}$
r/q	Geometric shunt impedance (Ω/m)	82.7	82.7	82.7
L	Electrical length (m)	0.1	0.1154	0.025
G	Geometry factor (Ω)	287	287	287

Table 3.2: *Important parameters when calculating the cavity excitation curve.*

cations introduced to perform the atmospheric plasma treatment.

1.5 GHz cavities cryogenic infrastructure

The photograph depicted in figure 3.2 represents the insert to measure the quality of 1.5, 1.3 (1/3 cells) superconducting cavities.

During the test, the cavity has to be cooled at cryogenic temperatures in order to reach the superconducting state (Nb transition temperature (T_c) is equal to 9.2 K).

The rf testing facility of the laboratory includes four apertures which can host a cryostat. Three of them are used to test QWRs and single cell TESLA type cavity. This kind of cryostat can hold 100 liters of liquid helium. The fourth one has been thought to measure multicell TESLA type cavities and can be filled with 400 liters of helium. The last has been designed for operating at 4.2 K and 1.8 K at the maximum power of 70 W.

The He vessel (figure 3.3) is constituted by three successive jackets: the most internal one contains helium gas (or it is pumped at low pressure), the middle one is used for liquid nitrogen and the third container is under vacuum to thermally insulate cryostat sides. The second chamber is connected to the liquid nitrogen tank placed outside the laboratory.

The upper part of the cryogenic infrastructure has been been equipped with a set of copper shields for thermal insulation. They are cooled with the recovery helium cold gas.

In order to reduce the cooling cost, a preliminary cooling is performed using the liquid nitrogen (*middle jacket*). Thus the He vessel is filled with Helium gas at a pressure of 1000 mBar, and the thermal contact between the He vessel and the liquid N₂ chamber is obtained filling the chamber in between with He gas at 200 mBar. When the temperature reaches 80 K, the He gas is removed and the transfer of liquid He at 4.2 K into the main vessel is started.

Usually the cavity is tested at 4.2 K and then at 1.8 K. The temperature of liquid helium can be lowered decreasing the chamber pressure. A pumping line takes away the vapor over the liquid and hence some liquid helium evaporates to compensate the drop pressure.

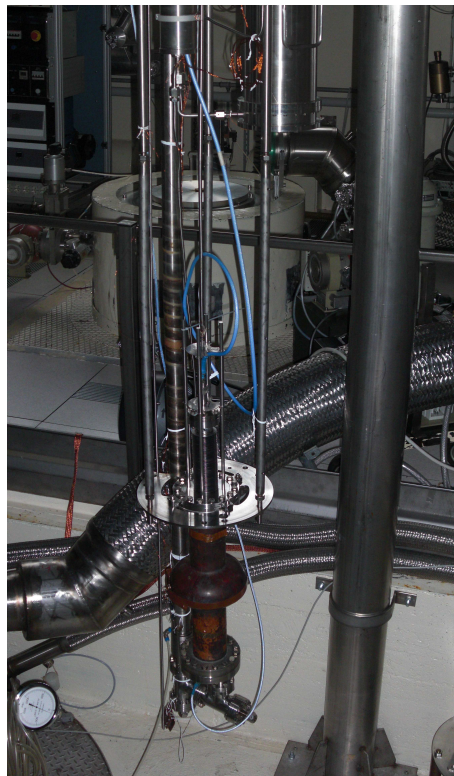


Figure 3.2: *The cryogenic infrastructure built to test 1.5, 1.3 (1/3 cells) . In the photograph a mono-cell resonator is connected to the stand. It is a Nb sputtered on Cu resonant structure. The process gas flows through the pumping line, from the top of the system (cryostat cover) to the upper flange of the cavity. The bottom flange of the resonator is the one described in figure 3.10: it houses the pickup probe antenna and a glassy window to verify what happens inside.*

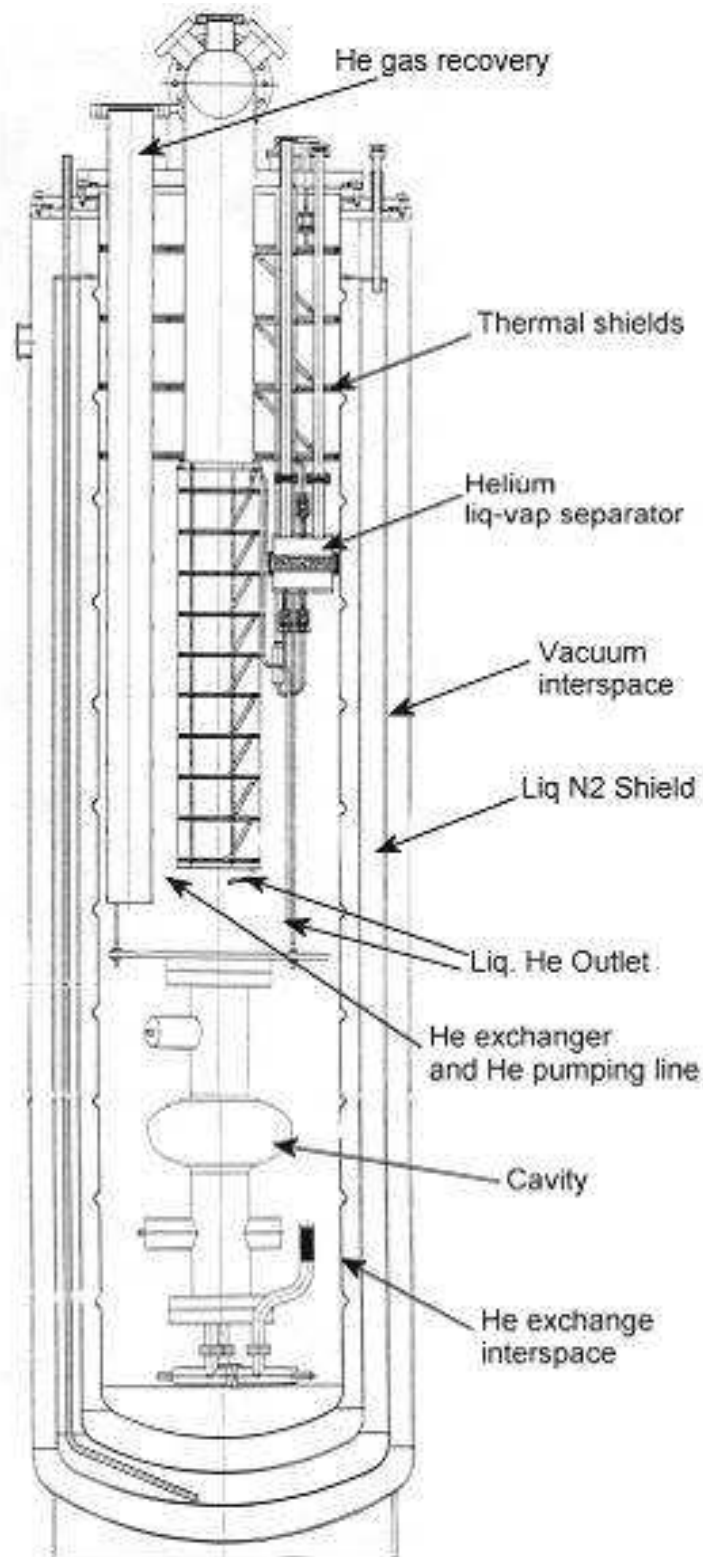


Figure 3.3: A schematic of the cryogenic infrastructure inserted in the cryostat used to test 1.5, 1.3 (1/3 cells) superconducting cavities. All the most important parts are contextually mentioned.

Furthermore a liquid helium supply at 1.8 K must be introduced in order to keep the level constant. This task is carried out by a heat exchanger, that utilize the cooling capacity of the return gas stream to cool down the incoming liquid. The cooled fluid is sent into a liquid/gas separator. The low temperature portion is taken apart by a sinter brass plate in the middle of the separator. The liquid flows by capillarity action towards the lower side while the gaseous phase remains on the upper part and it is used to refrigerate the copper shields. The stream of liquid is regulated by two valves which can be operated manually from the outside. By changing the pumping speed it is possible to set the evaporation rate and, in turn, the amount of power removed from the dewar. The bath pressure and temperature are regulated controlling the system pumping speed. Typically, a single cell cavity dissipates only few tens of watts during the test.

When the cavity is mounted on the cryogenic infrastructure for the cold test it is evacuated through the system sketched in figure 3.4.

The pumping unit is made of an oil free backing pump and a turbo-molecular pump.

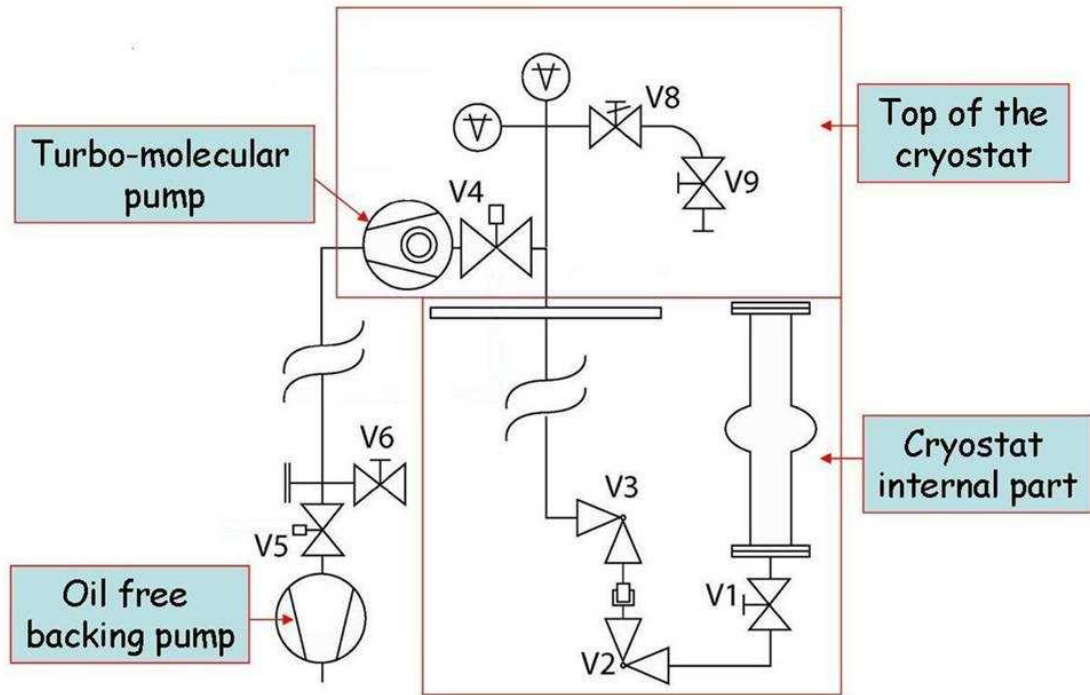


Figure 3.4: A schematic of the cavity pumping system.

Valve V5 is used to insulate the turbo pump in case of power failure. V6 is used for any eventual leak detection. V4 is the main gate valve. V7 allows the system venting (if the gate valve is closed). V8 and V9 (thought for helium conditioning) *constitute the processing gas inlet during an atmospheric plasma treatment*. The gas path starts at the top of the insert, it continues passing through the cavity and it stops at the resonator top flange. The last has been holed to weld a small pipe connected to a Swagelock assembly. When the

process gas is helium it has to be properly recovered (through the Lab automatic recovery system).

V3 allows leaving under vacuum the "fixed" part of the system, which is connected to the cavity by the VCR between V2 and V3.

The cryostat vacuum chamber has a long pipe connecting the pumps (at room temperature) to the cavity immersed in the liquid helium. In this situation the cavity itself acts as a cryogenic pump, while the low conductance of the pipe reduces the effective pumping speed of the upper pumps. It is thus advisable to evacuate the cavity before the mounting on the cryostat insert using a separated vacuum facility.

Finally, after an overnight baking and 8 hours of pumping the pressure is usually in the 10^{-9} mbar range.

6 GHz cavities cryogenic infrastructure

The stand we use to perform the rf tests of 6 GHz cavities has been recently built [27] and its global appearance is depicted in figure 3.5.

This insert is very compact: it has been conceived to enter a 450 or 250 l dewar neck.

Such an infrastructure permit us to significantly reduce the cryogenic power consumption, avoiding any loss during a helium transfer into a cryostat: a measurement performed at 4.2 K requires roughly 30 liters of liquid He.

On the 6 GHz stand top flange a few holes have been properly drilled to allow a way through for the two rf cables, the thermal probe and the vacuum line (figure 3.6). The most important thing to notice is the *all metal valve* placed to permit the *process gas to flow in* when necessary. All the technical details are deeply analyzed in [27]: I just want to underline the gas path starts at the top of the insert, it continues passing through the cavity and than it goes back to the stand upper part to be recovered.

There is a linear feedthrough (figure 3.6) that, together with the bellow connected on the upper cavity flange, permits the coupler antenna motion. It is surrounded by a metal structure used to fix the stand to the overhead traveling crane during the needed displacements. The rf cables connectors (N-type) are clearly visible too: they are embedded into two supports, thought to avoid their stresses or motions during the cavity measurement.

As shown in figure 3.7, to oversimplify the system assembling, the bottom part of it has been made completely independent: the small cavity can be mounted without the presence of the complete stand that would make the work complicated. The cavity is closed by two stainless steel flanges, on which the rf SMA connectors are welded. A 1.5 mm diameter indium wire is squeezed between these flanges and the cavity flat borders with eight stainless steel half round rings.

Four teflon coated vertical bar lines preserve the system alignment and prevent blockage problems due to the freeze-over of the bellow upper flange during the liquid helium insertion step.

The bottom part is covered by a μ -metal shield during the rf tests.

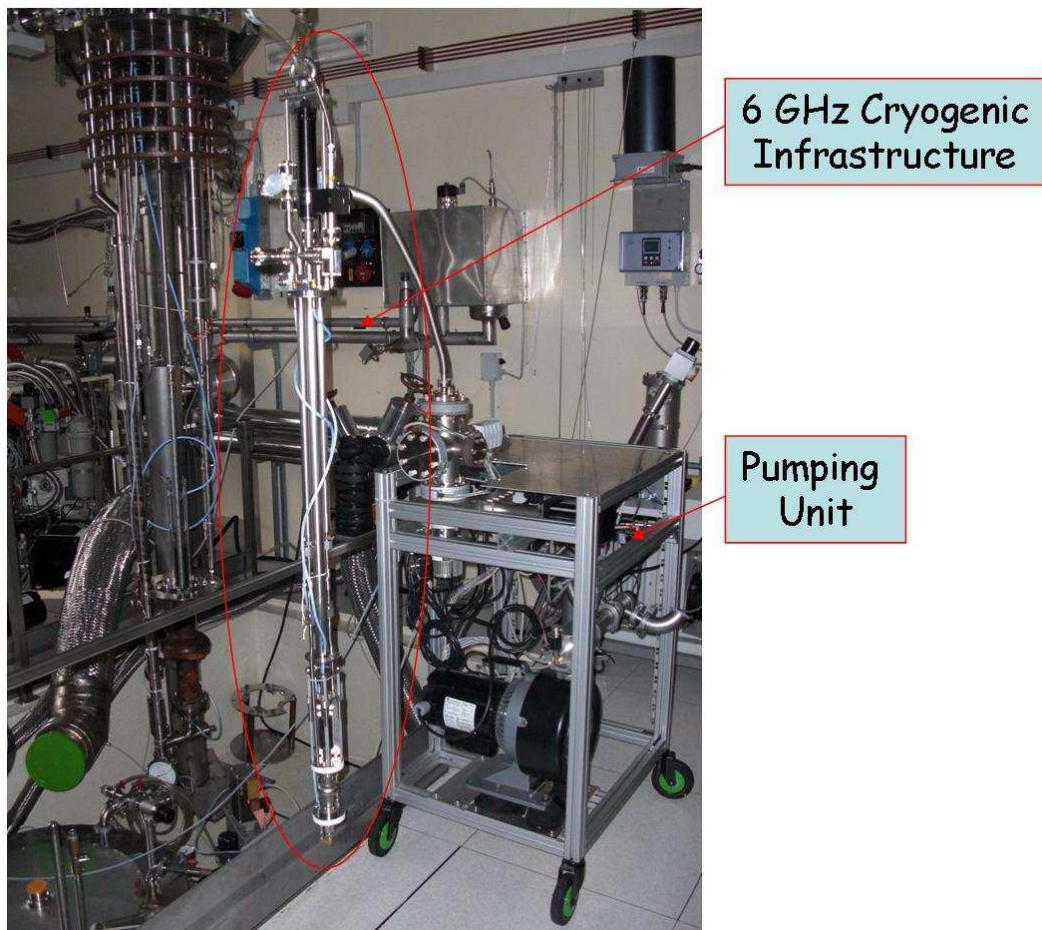


Figure 3.5: The cryogenic infrastructure built to test 6 GHz superconductive cavities. In the photograph a bulk niobium resonator is connected to the stand. The process gas flows (through the pumping line) from the top of the system to the small resonator, then it runs up again to be recovered. As a comparison look at the stand used for 1.5/1.3 GHz (on the left side of the photograph) to notice their different dimensions. The small 6 GHz testing apparatus has been designed to enter a 250/450 liters liquid helium dewar.

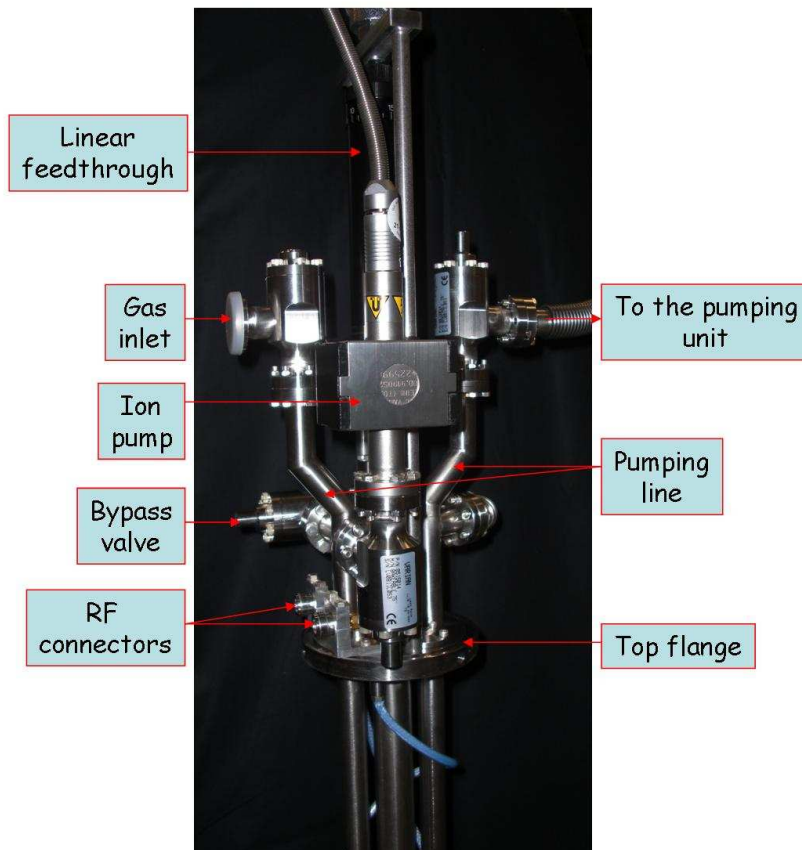


Figure 3.6: On the 6 GHz stand top flange a few holes have been properly drilled to allow a way through for the two rf cables, the thermal probe and the vacuum line. The most important thing to notice is the all metal valve placed to permit the process gas to flow in when necessary (all the technical details are deeply analyzed in [27]). The gas flows from the top of the insert, it continues passing through the cavity and than it goes back to the stand upper part (to be recovered).

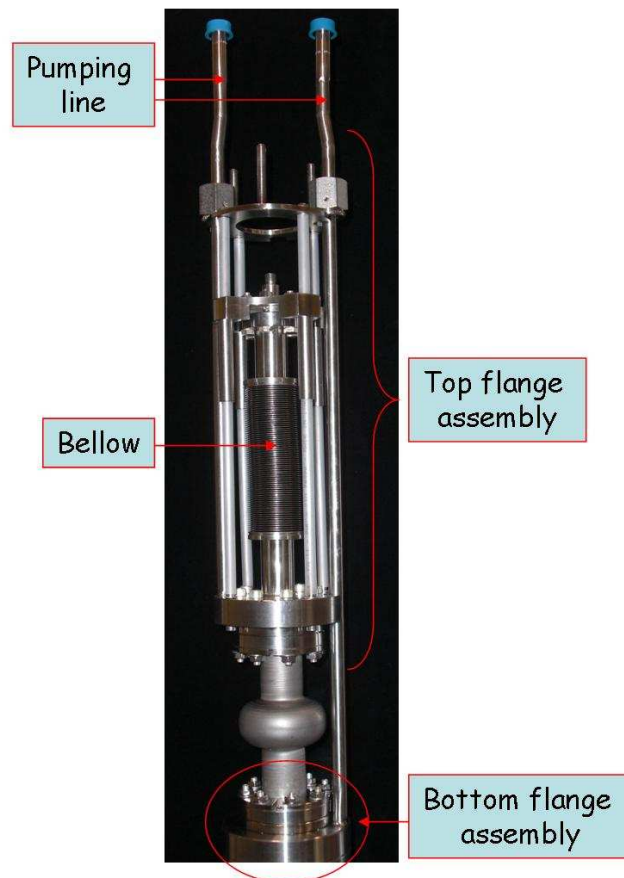


Figure 3.7: To oversimplify the system assembling, the bottom part of it has been made completely independent. The cavity is closed by two stainless steel flanges, on which the rf SMA connectors are welded. A 1.5 mm diameter indium wire is squeezed between these flanges and the cavity flat borders with eight stainless steel half round rings. Four teflon coated vertical bar lines preserve the system alignment and prevent blockage problems due to the freeze-over of the bellow upper flange during the liquid helium insertion step.

3.1.3 Procedure

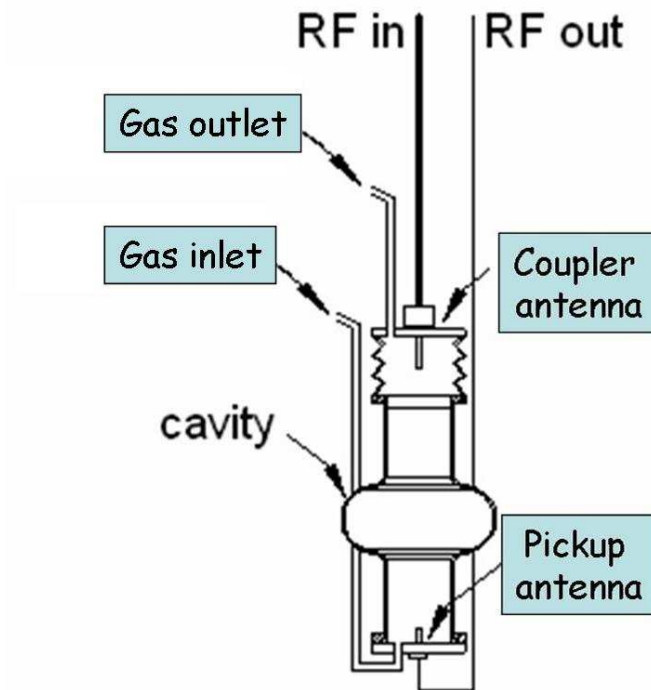


Figure 3.8: Experimental configuration for a typical resonance atmospheric plasma treatment.

First of all a rf tested resonator is needed so that the corresponding Q vs E_{acc} curve represents our *starting point*. As an example, a set of excitation curves of 1.5 GHz bulk niobium resonant cavities is depicted in figure 3.9. The quality factor is higher than 10^{10} while the accelerating field exceeds 30 MV/m.

The operative procedure we developed to perform the resonance atmospheric plasma treatment of a superconducting cavity is the following:

- The first thing to do is to get the warm critical coupling condition. Moving the coupler antenna and changing the loop phase, it is possible to minimize the reflected power determining the ideal matching condition ([23, 24]).
- The next step consists into the gas inlet and outlet opening while maintaining the rf power on. Usually it is necessary to set the proper matching condition again (slightly modifying the antenna position and the loop phase).
- The third important point is the power increasing until the plasma ignition.
- Then the resonance atmospheric plasma is kept on for the decided time interval (30 minutes is a typical process duration).
- rf power is switched off while the gas flux is hold stable. The resonant cavity has to be screwed up before closing the gas line and starting pumping again.

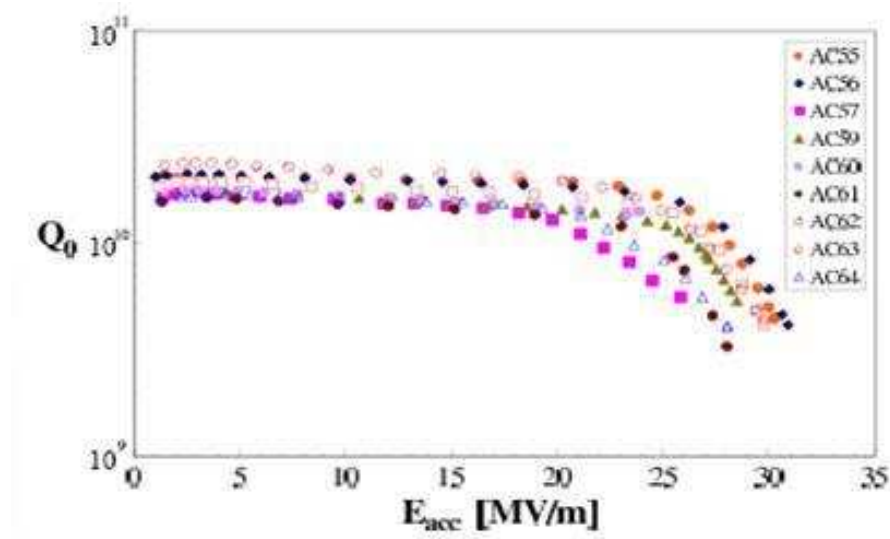


Figure 3.9: An example of a set of excitation curves of cavities (1-cell, 1.5 GHz) of TTF (Tesla Test Facility) production. Tests were done at 2 K [28].

- The last step is the cavity rf testing to compare the new characteristic to the previous data.

Comments

First of all it is necessary to work at (or near) the *critical coupling* condition to get the maximum electromagnetic field into the resonator cell. Let's visualize the Q vs E_{acc} curve: when the atmospheric plasma is ignited the quality value, the accelerating field (and obviously P_{pk}) decrease suddenly to prove it is consuming part of the forward power.

It is essential to avoid the Nb cleaned surface contamination due to the process gas. Ideally it has to be extra-pure. Furthermore the gas cylinder must be connected to the cryogenic infrastructure pipe line through electropolished stainless steel tubes. All the used connections have to be metallic and properly airtight.

Moreover we must be careful while using rf power. All the steps of the atmospheric plasma treatments have to be carefully monitored through an electromagnetic field probe [29].

3.2 1.5 GHz cavities

The gas inlet is on the bottom flange (*inlet flange*). The last is a CF 100 with two CF 35 flanges and the pickup probe entry (figure 3.10). One of the two CF 35 flanges is connected to the gas cylinder (through a proper transition) with a plastic tube. The other has been used as a window.

On the top flange (*outlet flange*) a bellow and four bars (teflon covered) are fixed to allow the coupler antenna movement. A hole has been drilled to weld a stainless steel electropolished piece of tube ended with a Swagelock assembly (figure 3.10). It's purpose is to make the process gas to flow out of the cavity.

Initially helium has been used and the atmospheric plasma is depicted in figure 3.11.

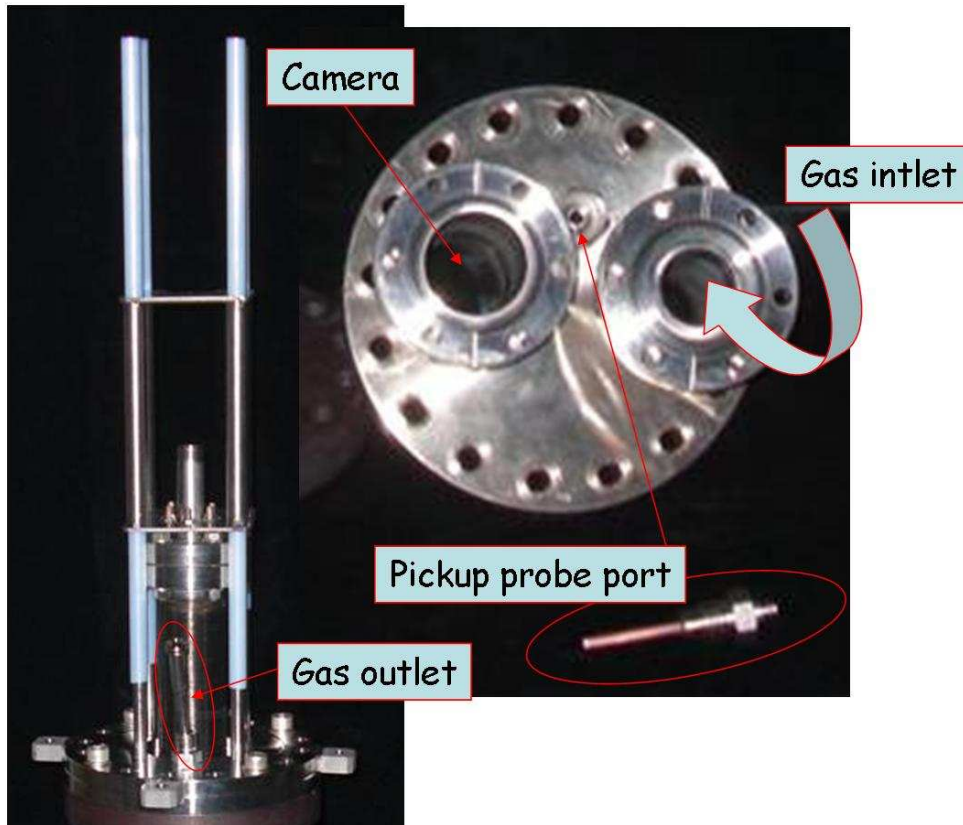


Figure 3.10: The bottom flange of the 1.5 GHz resonator (on the right picture) houses two CF 35 flanges : the first is used to fix a glassy window to verify what happens inside the cavity, the other one works as the process gas inlet. The pickup probe antenna entry is placed on the same flange too. On the outlet flange a bellow and four bars (teflon covered) are fixed to allow the coupler antenna movement. A stainless steel electropolished piece of tube ended with a Swagelock assembly is welded too to make the process gas flowing out.

It has been photographed from the *inlet flange* (through a glassy window plus a protective wire netting). As expected it is placed in the high field zone and it looks sphere-shaped. It maintains an *equilibrium position* until the flux flow is *sufficiently low*. We decided not to use a mass flow controller but just the cylinder adaptor to regulate the gas stream. When it becomes *high*, the *plasma ball* starts moving randomly, touching the cavity internal surface.

As a second attempt we decided to use a scrap cavity, just to perform a feasibility study. It is made of stainless steel and it has been built to control the plasma appearance during a magnetron sputtering deposition experiment. It is characterized by a CF 35 flange welded

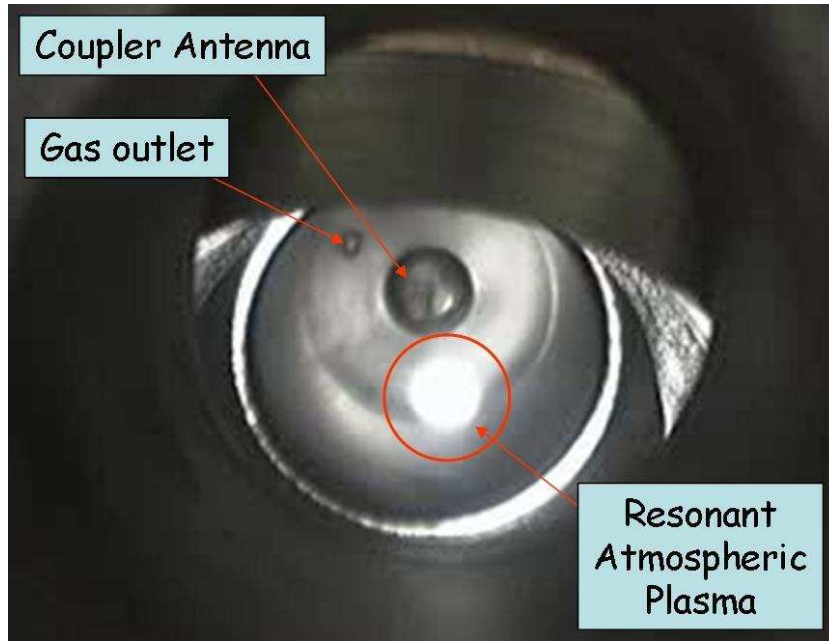


Figure 3.11: Helium flux moves from the bottom flange to the top one. The phenomenon has been observed from the glassy window fixed to the 1.5 GHz cavity lower side. The ignited plasma looks sphere-shaped. As expected it is placed in the high field zone.

on the cavity cell (figure 3.12).

The basic idea is to take the chance to observe the ignited plasma sideways and from the bottom part of the resonator.

Figure 3.13 represents the *cigar-shaped* plasma we obtained using Ar as the gas process. The ignited plasma is smaller than the He one. Observing the phenomenon sideways it is evident the electromagnetic field distribution influences the resonance plasma shape.

In the following table some useful data have been reported. It is a typical example of the experiments we performed.

We have a 500 W amplifier and, because of the high power, the rf connector zone (top of

f	1.492 GHz
P_i	190 W
P_{ref}	80 W

Table 3.3: Common parameters measured during a plasma process.

the bellow fixed to the *outlet flange*) is cooled through a fan.

3.3 6 GHz cavities

Having at our disposal the "6 GHz powerful tool", we decided to switch on the resonance atmospheric plasma into a small resonator. In this way it becomes extremely easy



Figure 3.12: For the first attempts, the resonance atmospheric plasma has been observed (through a protective wire netting) from a glassy window fixed to the 1.5 GHz cavity cell.

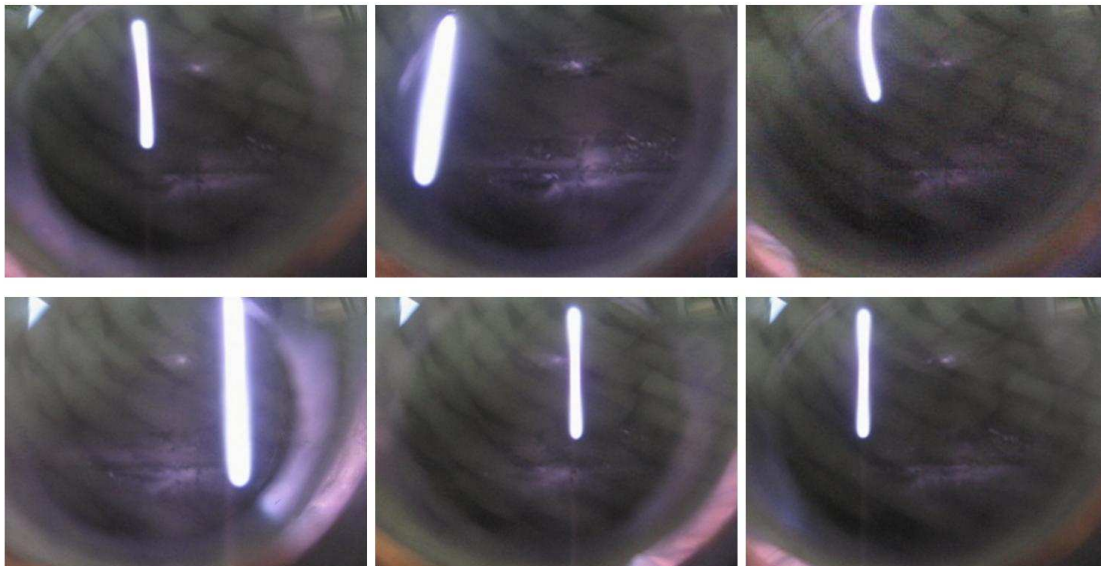


Figure 3.13: Argon flux moves from the top flange to the bottom one. The phenomenon has been observed (through a protective wire netting) from a glassy window fixed to the cavity cell. The ignited plasma looks cigar-shaped. As expected it is placed in the high field zone. It moves in an uncontrolled way and it often stops in correspondence to defects of the test resonator walls.

to treat the surface and verify its effects on the cavity performance.

A resonance TM010 mode atmospheric plasma has been ignited inside a bulk Nb 6 GHz resonator at room temperature under an helium flux of approximately 15 l/minute.

The experimental apparatus used to treat the cavity is illustrated in figure 3.8, during the plasma treatment helium was fluxed inside the cavity through the pumping line and extracted from the cavity by a dedicated line.

The plasma power has been kept constant at 8 W and during the process the cavity temperature was stable at 50°C. We've done three treatments in succession:

- two of thirty minutes and
- the last of 10 minutes of ATM plasma plus 10 minutes of ultrasonic cleaning,

in order to investigate the effects of sonic waves on an atmospheric plasma treated surface. Q_0 and Q vs. E_{acc} were measured after each treatment session.

The Nb 6 GHz cavity has been initially prepared with 1 hour BCP 1:1:2, 1 hour EP, 4 hours baking at 900 °C with Ti used to getter hydrogen and oxygen and finally with a BCP 1:1:2 for 3 minutes to get rid of the Ti contamination. The cavity has then been measured showing a starting Q_0 equal to 7×10^6 .

After the initial standard treatments the cavity underwent:

- Thirty minutes of resonance atmospheric plasma with just helium as process gas and the Q_0 increased to 2×10^7 .
- A successive second treatment of 30 minutes on the same cavity didn't show any further improvement.
- A third plasma treatment has been carried on for ten minutes and it has been followed by and ultrasonic rinsing with deionized water. The Q_0 rose to $2,8 \times 10^7$, the error for all the measures being 10%.

The increment in Q_0 has been confirmed also by the decay time that passed from 1×10^{-4} s to $2,7 \times 10^{-4}$ s (after the first and second treatment) and finally to $3,7 \times 10^{-4}$ s after the ultrasonic rinsing.

The electric field gradient has also been improved going from 2,5 MV/m to 3,7 MV/m. The results are reported in figure 3.14 and in figure 3.15.

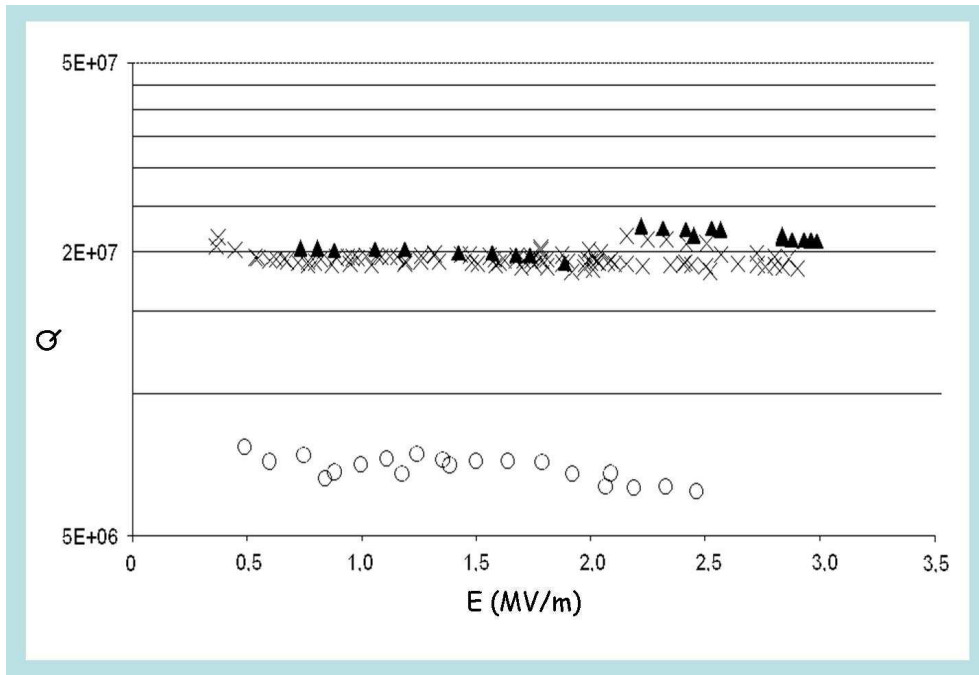


Figure 3.14: Q vs. E_{acc} of the Nb 6 GHz cavity treated with atmospheric resonance plasma. "o" starting situation; "x" 30 minutes plasma treatment; " Δ " 60 minutes plasma treatment.

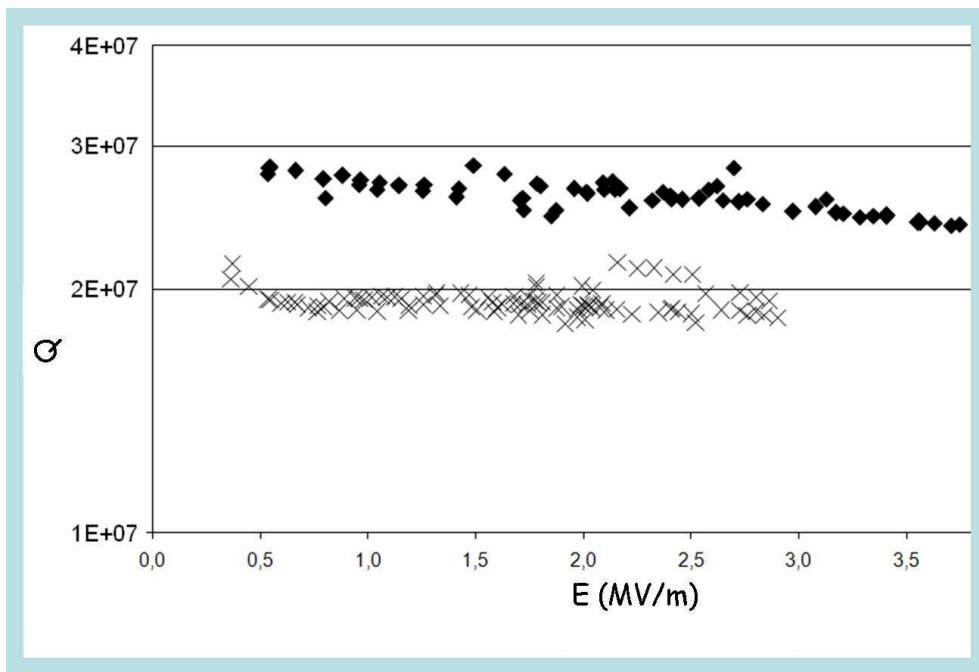


Figure 3.15: Q_0 increment after the third treatment. "x" 30 minutes plasma treatment; " \diamond " 10 minutes plasma plus 10 minutes ultrasonic rinsing.

Chapter 4

Discussion

Atmospheric-pressure plasma treatment is an emerging, very versatile and inexpensive technique used in a variety of surface processes such as dry etching, surface treatments and modification of surface wettability.

We have applied a resonance atmospheric plasma cleaning step to further clean a 6 GHz Nb seamless cavity observing an increment in the Q_0 from 7×10^6 to 2×10^7 .

We have started the investigation of a simple, reliable and easy to set up atmospheric plasma treatment. Looking at the experimental results the most probable explanation is that *helium plasma* changes the energy of the cavity internal surface. After the treatment it becomes extremely *hydrophilic*.

The changing of a surface hydrophilicity/hydrophobicity (and hence water wettability) is a mechanism widely studied in the nanotechnology field and in material science: plasma treatment is one of the most versatile techniques used for such surface modification. It is also widely used to alter the surface properties of materials in a number of applications like improving adhesion of coatings to metals and polymers [30], increasing wettability and printability of polymers [31, 32], enhancing biocompatibility of implants [33], and in the manufacturing of semiconductor devices [34, 35].

The increased wettability due to the plasma action on the inner cavity surface has proved to enhance the beneficial action of water rinsing pushing the Q_0 value further up close to 3×10^7 .

Water wettability

The individuation and construction of the right plasma source by which it would have been possible and easy to treat the internal part of an accelerating cavity has been studied a bit in this Lab and the sources, characterized by a different plasma power, ignition mechanism and plasma shape, have been already described in [36].

The effect of a 5 minutes treatment on different substrates has been analyzed using the sessile drop method and measuring the contact angle (C.A.) of a 300 μl deionized water droplet. An increment in hydrophilicity and wettability has been evidenced by the

decrement in the contact angle, phenomenon that has been observed for all the analyzed substrates.

The C.A. modifications were similar with all the atmospheric plasma sources that have been studied and all of them presented a very similar optical emission spectrum. There were signals of helium, the carrier gas, and of oxygen and nitrogen present as contaminants. The increment in water wettability (hydrophilicity) could be due to the oxidation of carbon contaminants on the surface by the chemical activated hydroxide anion OH^- and radical oxygen O^\bullet but also to the creation of polar sites by the charged species formed in the plasma. Another explanation, related to the former one, is that the surface energy increased after the plasma treatment and the formation of a solid-liquid contact area was energetically favorite if compared to the solid-gas one. The changing in surface energy could also be responsible for a different interaction between the solid and the adsorbed gases that could desorb leaving a cleaner surface.

Resonance plasma

The shape of the plasma inside the cavity is determined by the electric and magnetic field

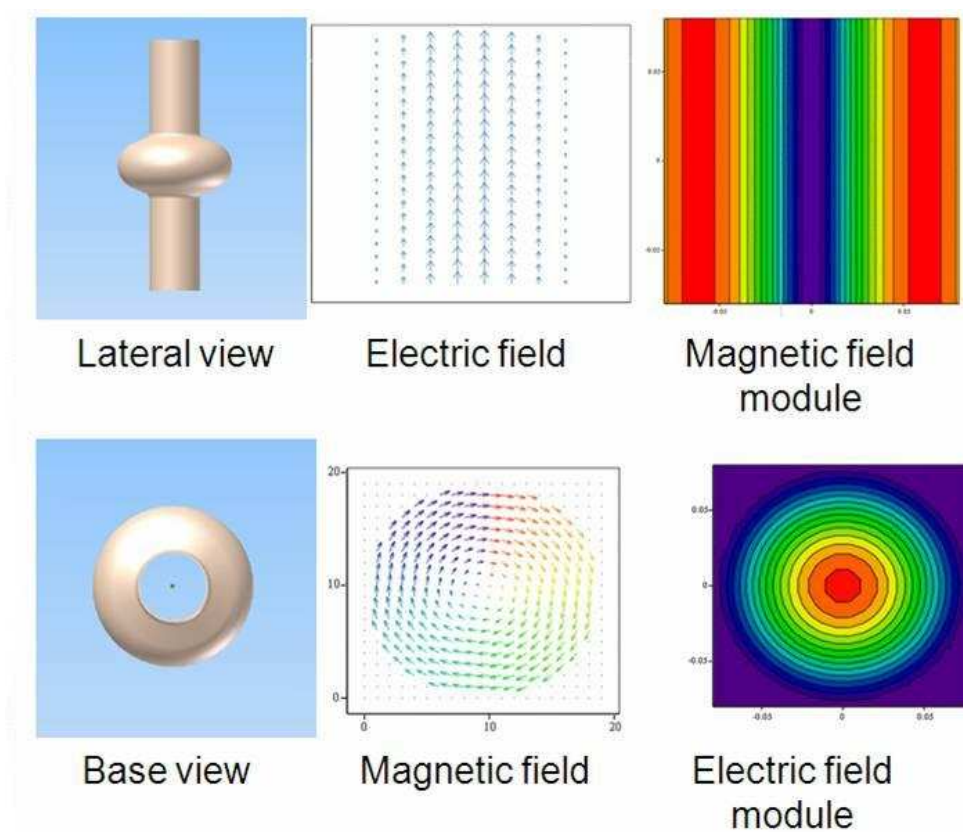


Figure 4.1: *Magnetic and electric field distribution of the fundamental mode TM_{010} referred to a tesla type cavity.*

of the excited fundamental mode. The electric field module is the highest in the center of the cell while the magnetic field has its highest module in the border region of the cell, as

reported in figure 4.1.

With this electric and magnetic field distribution, the plasma assume a *cigar shape*: it is centered in the cavity cell (with its main axis parallel to the resonator one) and has the capacity to uniformly treat its internal surface.

Surfactants analogy

Surfactants that are present in soaps have the property to increase the surface wettability by shielding the water intermolecular interactions and hence decreasing the surface tension. Therefore water with surfactants can spread better on the surface that has to be cleaned. The cleaning action can be more effective also in the small interstitial volumes which would not be treated by a liquid with low wettability and high surface tension. So *high wettability* means *high interaction* between the solid and the liquid. This *high interaction* can be achieved by using atmospheric plasma too. The main advantage is it doesn't leave contaminants on the surface as it happens with soaps.

In our experiment the cleaning process has been enhanced by the ultrasonic rinse whose action has been made more effective by the high wettability of the cavity internal surface.

Chapter 5

Conclusions and future plan

More experiments will be carried on 6 GHz cavities exploring the effects of rinsing time and helium flux variation.

The cleaning process will be also studied on 1.5/1.3 GHz cavities in order to analyze what happens when the ratio ionization volume/cell surface decreases. It is easy to think the *plasma ball* has to be maintained close enough to the surface to be treated: as already discussed, it moves randomly when the flux flow is high. It is mandatory to understand everything about the gas stream dynamic and to make the plasma to *touch* the resonator internal surface.

Moreover it could be interesting to try to ignite a resonance atmospheric plasma into a multi-cell cavity.

The chemical activation by atmospheric plasma gives also the possibility to add reactive gases in the carrier flux and investigate the etching rate due to chemical activated fluorine ions coming from mixture of CF_4 , NF_3 with and without oxygen. These gas mixtures have already successfully been used to etch Nb in the semiconductor industry for the realization of Josephson junctions ([37, 38]).

The following step will consist in the realization of different atmospheric configurations as corona plasma, plasma jet and torch.

Appendix A

Basics of superconducting radio-frequency cavities

In this chapter we give an overview of the basics of superconducting cavities. We start by discussing the electrodynamics of radiofrequency (rf) cavities, the accelerating mode and the general expressions used to describe power dissipation. Although later we focus exclusively on superconducting cavities, this section apply equally well to both normal and superconducting resonant structures.

In the second part we introduce the rudiments of superconductivity. In particular, we will illustrate why superconducting cavities dissipate a small, but finite amount of power despite the fact that superconductors carry dc currents without losses. We will also explain the fundamental magnetic field limitation of superconducting cavities.

This chapter is not designed to give a deep description of the theory of cavities: we will just emphasize the aspects needed to understand this report. For further information the reader is referred to numerous texts that give an excellent review of the subject (see, for example [1, 39]).

A.1 Cavity fundamentals and cavity fields

A.1.1 Radio-frequency fields in cavities

The rf field in cavities are derived from the eigenvalue equation

$$\left(\nabla^2 - \frac{1}{c^2} \frac{\partial^2}{\partial t^2} \right) \begin{pmatrix} E \\ H \end{pmatrix} = 0 \quad (\text{A.1})$$

which is obtained by combining Maxwell's equations [40]. It is subject to the boundary conditions

$$\hat{n} \times \mathbf{E} = 0 \quad (\text{A.2})$$

and

$$\hat{n} \cdot \mathbf{H} = 0 \quad (\text{A.3})$$

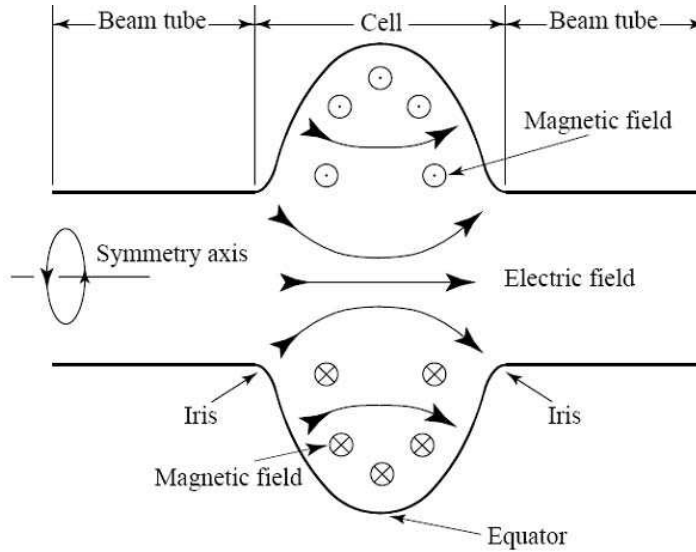


Figure A.1: Schematic of a generic speed-of-light cavity. The electric field is strongest near the symmetric axis, while the magnetic field is concentrated in the equator region.

at the cavity walls. Here \hat{n} is the unit normal to the rf surface, c is the speed of light and \mathbf{E} and \mathbf{H} are the electric and magnetic field respectively. In cylindrically symmetric cavities, such as the pillbox shape, the discrete mode spectrum given by A.1 splits into two groups, transverse magnetic (TM) modes and transverse electric (TE) modes. For TM modes the magnetic field is transverse to the cavity symmetry axis whereas for TE modes it is the electric one to be transverse. For accelerating cavities, therefore, only TM modes are useful.

Modes are classified as TM_{mnp} , where integers m , n , and p count the number of sign changes of E_z in the Φ , ρ , and z directions respectively. Only TM_{0np} ($n = 1, 2, 3, \dots; p = 0, 1, 2, \dots$) modes have a non vanishing longitudinal electric field on axis, and the TM_{010} mode is used for acceleration in most cavities.

The typical shape of speed of light cavities [1] is shown in Figure A.1. The electric field of the TM_{010} mode is greatest at the irises and near the symmetry axis, while the magnetic field is concentrated in the equator region. The geometry of the cell and the addition of beam tubes make it very difficult to calculate the fields analytically, and one reverts to numerical simulations with codes such as SUPERFISH to obtain the field profiles [25]. Although TM modes acquire a finite H_z due to the perturbative effect of the beam tubes, the main characteristic of the TM modes are preserved, and one still uses the TM_{mnp} classification scheme to identify modes.

A.1.2 The accelerating field

The accelerating voltage (V_{acc}) of a cavity is determined by considering the motion of a charged particle along the beam axis. For a charge q , by definition,

$$V_{acc} = \left| \frac{1}{q} \times \max \text{ energy gain possible during transit} \right| \quad (\text{A.4})$$

We use 6 GHz speed of light structures in our tests, and the accelerating voltage is therefore given by

$$V_{acc} = \left| \int_{z=0}^{z=d} E_z(\rho = 0, z) e^{\frac{i\omega_0 z}{c}} dz \right| \quad (\text{A.5})$$

where d is the length of the cavity and ω_0 is the eigenfrequency of the cavity mode under consideration. Frequently, one quotes the accelerating field E_{acc} rather than V_{acc} . The two are related by

$$E_{acc} = \frac{V_{acc}}{d} \quad (\text{A.6})$$

With single cell cavities the choice of d is somewhat ambiguous, since the beam tubes can be made arbitrarily long. Hence E_{acc} is not uniquely defined. Frequently one therefore calculates E_{acc} for an equivalent infinite periodic structure and quotes its E_{acc} for the single cell.

A.1.3 Peak surface fields

When considering the practical limitations of superconducting cavities, two fields are of particular importance: the peak electric surface field (E_{pk}) and the peak magnetic surface field (H_{pk}). In most cases these fields determine the maximum achievable accelerating gradient in cavities. In the ones we have (6 GHz speed of light structures), the surface electric field peaks near the irises, and the surface magnetic field is at its maximum near the equator. To maximize the potential cavity performance, it is important that the ratios of E_{pk}/E_{acc} and H_{pk}/E_{acc} be minimized.

In an ideal pillbox cavity, the ratios are given by

$$\frac{E_{pk}}{E_{acc}} = \frac{\pi}{2} = 1.6 \quad (\text{A.7})$$

$$\frac{H_{pk}}{E_{acc}} = 30.5 \quad \frac{Oe}{MV/m} \quad (\text{A.8})$$

The addition of beam tubes increases these values. For example, the ratios of monocell TESLA-type cavities are

$$\frac{E_{pk}}{E_{acc}} = 1.83 \quad (\text{A.9})$$

$$\frac{H_{pk}}{E_{acc}} = 45 \quad \frac{Oe}{MV/m} \quad (\text{A.10})$$

These values were obtained by solving for the fields in the TM010 mode numerically with the code SUPERFISH ([25], Chapter ??).

A.1.4 Power dissipation and the cavity quality

To support the electromagnetic fields, currents flow in the cavity walls at the surface. If the walls are resistive, the currents dissipate power. The resistivity of the walls is characterized by the material dependent surface resistance R_S which is defined via the power P_d dissipated per unit area:

$$\frac{dP_d}{da} = \frac{1}{2} R_S |\mathbf{H}^2| \quad (\text{A.11})$$

In this case, \mathbf{H} is the local surface magnetic field. In the next section we will show that superconductors are not completely lossless at rf frequencies, so that the previous formula applies equally to normal conductors and superconductors.

Directly related to the power dissipation is an important figure of merit called the cavity quality (Q_0). It is defined as

$$Q_0 = \frac{\omega_0 U}{P_d} \quad (\text{A.12})$$

U being the energy stored in the cavity. The Q_0 is just 2π times the number of rf cycles it takes to dissipate an energy equal to that stored in the cavity.

For all cavity modes, the time averaged energy in the electric field equals that in the magnetic field, so the total energy in the cavity is given by

$$U = \frac{1}{2} \mu_0 \int_V |\mathbf{H}|^2 dv = \frac{1}{2} \epsilon_0 \int_V |\mathbf{E}|^2 dv \quad (\text{A.13})$$

where the integral is taken over the volume of the cavity. Equation A.11 yields the dissipated power

$$P_d = \frac{1}{2} \int_S R_S |\mathbf{H}|^2 ds \quad (\text{A.14})$$

where the integration is taken over the interior cavity surface. (By keeping R_S in the integral we have allowed for a variation of the surface resistance with position.) Thus one finds for Q_0 :

$$Q_0 = \frac{\omega_0 \mu_0 \int_V |\mathbf{H}|^2 dv}{\int_S R_S |\mathbf{H}|^2 ds} \quad (\text{A.15})$$

The Q_0 is frequently written as

$$Q_0 = \frac{G}{\overline{R_S}} \quad (\text{A.16})$$

where

$$G = \frac{\omega_0 \mu_0 \int_V |\mathbf{H}|^2 dv}{\int_S |\mathbf{H}|^2 ds} \quad (\text{A.17})$$

is known as the geometry constant, and

$$\overline{R_S} = \frac{\int_S R_S |\mathbf{H}|^2 ds}{\int_S |\mathbf{H}|^2 ds} \quad (\text{A.18})$$

is the mean surface resistance (weighted by H^2). For the 6 GHz cavities we studied $G = 287 \Omega$.

List of Tables

3.1	RF variables	32
3.2	Cavity rf parameters	36
3.3	RF variables	47

List of Figures

1.1	<i>A seamless Tesla Type bulk niobium 6 GHz cavity. Spun resonators don't need welding (even for flanges).</i>	2
1.2	<i>Spinning of a seamless multicell resonator from a circular blank.</i>	2
2.1	<i>Evolution of the plasma temperature (electrons and heavy particles) with the pressure in a mercury plasma arc.</i>	11
2.2	<i>Principle of a Corona discharge and a hollow needle to plate discharge (left: positive needle, right: negative needle).</i>	13
2.3	<i>Principle of dielectric barrier discharge (picture: a non equilibrium diffuse plasma at atmospheric pressure).</i>	14
2.4	<i>Principle of arc plasma torches (left: current-carrying arc; right: transferred arc).</i>	15
2.5	<i>RF plasma torch.</i>	15
2.6	<i>Left: cold plasma torch design. Right: barrier torch design.</i>	16
2.7	<i>APPJ design.</i>	17
2.8	<i>A schematic diagram of continuous corona discharge system for wool and mohair.</i>	18
2.9	<i>A schematic diagram of continuous corona system for Polypropylene Fiber Tow designed by Sherman Treaters [8].</i>	19
2.10	<i>Hydrophilic treatment of blood filters, capillaries (upper photograph): another and specially developed activation process can be used to make the surface hydrophilic. This permanently hydrophilic character is used to give woven, and non woven textiles the capability to be used as blood filter or filtering membranes for specific applications. Applications are micro filtration systems based on these textiles or capillaries: blood filters, dialysis filter systems etc. Hydrophobic treatment of non woven PP (bottom photograph): by using semi-continuous textile treaters it is possible to plasma polymerize the surface of non woven and other textiles so that they become hydrophobic of nature. A lot of industrial users are looking to replace their conventional techniques or improve the final result by using plasma technology. Applications are oleophobic or hydrophobic treatment of paper, tissues and filter elements.</i>	21

- 2.11 *To promote the Research and the Technological Transfer in the field of Plasma Applications, the University of Milano-Bicocca, together with the Regione Lombardia and the Fondazione Cariplo, supported the creation of a Centre of Excellence on Plasma Applications. The Centre of Excellence PLASMAPROMETEO was established on February 12 th 2004 on the basis of an agreement between the University of Milano-Bicocca and the Regione Lombardia. The aims of the Centre is to promote Technological Transfer and training to Small Medium Enterprises. (<http://www.plasmaprometeo.unimib.it/history.php>) 25*
- 2.12 *Tantec has been offering cutting-edge and environmentally-friendly Plasma and Corona surface treatment equipment for over thirty years. Tantec develops, manufactures and markets innovative equipment worldwide for Plasma and Corona surface treatment of plastic components. Atmospheric Plasma treating system provides an economical solution for the cleaning and activation of complex surfaces before further processing. Component preparation is an important step prior to bonding, painting, varnishing and coating processes. 27*
- 2.13 *The mobile phone housing is cleaned by a rotating plasma jet prior to painting. Vehicle manufacturer has been using Openair plasma for pretreating plastic surfaces. Switches with laser-etched symbols, high-gloss decorative strips and covers, scratch resistant displays and glittering fascias, ventilator grilles or glove compartments even plastic parts in the interiors of automobiles can be pretreated using plasma. 28*
- 3.1 *Input coupler arrangement used to couple rf power into the cavity. 33*
- 3.2 *The cryogenic infrastructure built to test 1.5, 1.3 (1/3 cells) . In the photograph a mono-cell resonator is connected to the stand. It is a Nb sputtered on Cu resonant structure. The process gas flows through the pumping line, from the top of the system (cryostat cover) to the upper flange of the cavity. The bottom flange of the resonator is the one described in figure 3.10: it houses the pickup probe antenna and a glassy window to verify what happens inside. 37*
- 3.3 *A schematic of the cryogenic infrastructure inserted in the cryostat used to test 1.5, 1.3 (1/3 cells) superconducting cavities. All the most important parts are contextually mentioned. 38*
- 3.4 *A schematic of the cavity pumping system. 39*
- 3.5 *The cryogenic infrastructure built to test 6 GHz superconductive cavities. In the photograph a bulk niobium resonator is connected to the stand. The process gas flows (through the pumping line) from the top of the system to the small resonator, then it runs up again to be recovered. As a comparison look at the stand used for 1.5/1.3 GHz (on the left side of the photograph) to notice their different dimensions. The small 6 GHz testing apparatus has been designed to enter a 250/450 liters liquid helium dewar. 41*

3.6	<i>On the 6 GHz stand top flange a few holes have been properly drilled to allow a way through for the two rf cables, the thermal probe and the vacuum line. The most important thing to notice is the all metal valve placed to permit the process gas to flow in when necessary (all the technical details are deeply analyzed in [27]). The gas flows from the top of the insert, it continues passing through the cavity and than it goes back to the stand upper part (to be recovered).</i>	42
3.7	<i>To oversimplify the system assembling, the bottom part of it has been made completely independent. The cavity is closed by two stainless steel flanges, on which the rf SMA connectors are welded. A 1.5 mm diameter indium wire is squeezed between these flanges and the cavity flat borders with eight stainless steel half round rings. Four teflon coated vertical bar lines preserve the system alignment and prevent blockage problems due to the freeze-over of the bellow upper flange during the liquid helium insertion step.</i>	43
3.8	<i>Experimental configuration for a typical resonance atmospheric plasma treatment.</i>	44
3.9	<i>An example of a set of excitation curves of cavities (1-cell, 1.5 GHz) of TTF (Tesla Test Facility) production. Tests were done at 2 K [28].</i>	45
3.10	<i>The bottom flange of the 1.5 GHz resonator (on the right picture) houses two CF 35 flanges : the first is used to fix a glassy window to verify what happens inside the cavity, the other one works as the process gas inlet. The pickup probe antenna entry is placed on the same flange too. On the outlet flange a bellow and four bars (teflon covered) are fixed to allow the coupler antenna movement. A stainless steal electropolished piece of tube ended with a Swagelock assembly is welded too to make the process gas flowing out.</i>	46
3.11	<i>Helium flux moves from the bottom flange to the top one. The phenomenon has been observed from the glassy window fixed to the 1.5 GHz cavity lower side. The ignited plasma looks sphere-shaped. As expected it is placed in the high field zone.</i>	47
3.12	<i>For the first attempts, the resonance atmospheric plasma has been observed (through a protective wire netting) from a glassy window fixed to the 1.5 GHz cavity cell.</i> .	48
3.13	<i>Argon flux moves from the top flange to the bottom one. The phenomenon has been observed (trough a protective wire netting) from a glassy window fixed to the cavity cell. The ignited plasma looks cigar-shaped. As expected it is placed in the high field zone. It moves in an uncontrolled way and it often stops in correspondence to defects of the test resonator walls.</i>	48
3.14	<i>Q vs. E_{acc} of the Nb 6 GHz cavity treated with atmospheric resonance plasma. "o" starting situation; "x" 30 minutes plasma treatment; "△" 60 minutes plasma treatment.</i>	50
3.15	<i>Q_0 increment after the third treatment. "x" 30 minutes plasma treatment; "◇" 10 minutes plasma plus 10 minutes ultrasonic rinsing.</i>	50
4.1	<i>Magnetic and electric field distribution of the fundamental mode TM010 referred to a tesla type cavity.</i>	52

- A.1 *Schematic of a generic speed-of-light cavity. The electric field is strongest near the symmetric axis, while the magnetic field is concentrated in the equator region. . . .* 58

Bibliography

- [1] H. Padamsee, J. Knoblock, H. T., RF Superconductivity for Accelerators, Wiley and Sons, New York, 1998.
- [2] P. Bernard, et al., Proceedings of the 1992 European Particle Accelerator Conference, edited by E.H. Henke et al. Editors Frontiers (1992) 1269.
- [3] N. Pupeter, Proceedings of the 7th Workshop on RF Superconductivity, edited by B. Bonin, Gif-sur-Yvette, France (1995) 67.
- [4] K. e. a. Saito, Proceedings of the 6th workshop on RF Superconductivity, edited by R.M. Sundelin, CEBAF, Newport News (1994) 1151.
- [5] J. Graber, Nucl. Instrum. Methods Phys. Res. A (1994) 572.
- [6] C. e. a. Crawford, Part. Accel. 1 (1995) 49.
- [7] C. Tendero, C. Tixier, P. Tristant, J. Deasmaison, P. Leprince, Spectrochimica Acta B 61 (2006) 2–30.
- [8] Y. Hwuang, Characterization of atmospheric pressure plasma interactions with textile/polymer substrates, PhD Thesis, 2003.
- [9] G. Abbot, G. Robinson, Textile Research Journal 47(2) (1977) 199–202.
- [10] S. Meiners, J. Salge, E. Prinz, F. Forster, Surface and Coatings Technology 98 (1998) 1121–1127.
- [11] S. Kanazawa, M. Kogoma, T. Moriwaki, S. Okazaki, Journal of Physics D - Applied Physics 21 (1988) 838–840.
- [12] P. Tsai, L. Wadsworth, J. Roth, Textile Research Journal 67(5) (1997) 359–369.
- [13] T. Montie, K. Kelly-Wintenber, J. Roth, IEEE Transactions on Plasma Science 28(1) (2000) 41–50.
- [14] C. Tendero, C. Tixier, P. Tristant, J. Deasmaison, P. Leprince, 25th IEEE-ICOPS Paper 3B03 (1998) 178.
- [15] A. Bradley, J. Fales, Chemical Technology 1(4) (1971) 232–237.

-
- [16] Y. Iriyama, T. Yasuda, D. Cho, H. Yasuda, *Journal of Applied Polymer Science* 39 (1990) 249–264.
- [17] H. Wang, M. Rembold, J. Wang, *Journal of Applied Polymer Science* 49 (1993) 701–710.
- [18] M. McCord, Y. Hwang, L. Canup, M. Qiu, Y. Bourham, *Journal of Applied Polymer Science*.
- [19] W. Thorsen, R. Landwehr, *Textile Research Journal* 40(8) (1970) 688–695.
- [20] D. Biro, G. Pleizier, Y. Deslandes, *Journal of Applied Polymer Science* 47 (1993) 883–894.
- [21] T. Wakida, S. Tokino, S. Niu, M. Lee, H. Uchiyama, M. Kaneko, *Textile Research Journal* 63 (1993) 438–442.
- [22] P. Koulik, *Plasma Chemistry and Plasma Processing* 20 (2000) 159–161.
- [23] S. Deambrosis, 6 GHz cavities: a method to test A15 intermetallic compounds rf properties, PhD Thesis, 2008.
- [24] G. Lanza, New magnetron configurations for sputtering Nb thin films into Cu tesla-type superconducting cavities, PhD Thesis, 2008.
- [25] K. Halbach, R. Holsinger, *Particle Accelerators* 7 (1976) 213–222.
- [26] T. Powers, Proceedings of the 12th workshop on RF Superconductivity, Cornell University, Ithaca, NY, USA 0.
- [27] A. Rossi, A miniaturized 6 GHz infrastructure for cutting down the cost of RF superconducting research, Master Thesis, 2008.
- [28] L. Lilje, Experimental Investigations on Superconducting Niobium Cavities at Highest Radiofrequency Fields, PhD Thesis, 2001.
- [29] I. C. on Non-ionizing Radation Protection, *Health Physics* 74 (1998) 494–521.
- [30] E. Liston, L. Martinu, M. Wertheimer, *J. Adhesion Sci Technol.* 7 (1993) 1091–1127.
- [31] D. Briggs, Surface treatments for polyolefins, in: *Surface Analysis and Pretreatment of Plastics and Metals*, Applied Sciece Publishers, Essex, England, 1982.
- [32] S. Wu, Modifications of polymer surfaces: mechanism of wettability and bondability improvements, in: *Polymer Interface and Adhesion*, Marcel Dekker, New York, 1982.
- [33] P. Chu, J. Chen, L. Wang, N. Huang, *Mat. Sci. Eng.* 36 (2002) 143–206.

-
- [34] H. Schmid, B. Kegel, W. Petasch, G. Liebel, Proceedings of Joint 24th International Conference Microelectronics (MIEL) and 32nd Symposium Devcs Materials SD'96, Nova Gorcia, Slovenia 0 (1996) 17-35.
- [35] L. Lieberman, A. Lichtenberg, Principles of Plasma Discharges and Material Processing, Wiley, New York, 1994.
- [36] N. Patron, R. Baracco, L. Phillips, M. Rea, C. Roncolato, D. Tonini, P. V., Proceedings of the thin films workshop "pushing the limits of RFS", Legnaro, Italy 0.
- [37] M. Chen, R. Wang, J. Vac. Sci. Technol. A 1.
- [38] J. Sasserath, J. Vivalda, J. Vac. Sci. Technol. A 8.
- [39] H. Piel, CERN Accelerator School: Superconductivity in Particle Accelerators, In S. Turner editor, Hamburg, Germany, 1988.
- [40] J. Jackson, Classical Electrodynamics, Wiley and Sons, New York, 2nd edition, 1975.

